Chapter 2

Poly-harmonic Analysis of Raman and Mandelstam-Brillouin Scatterings and Bragg Reflection Spectra

Oleg G. Morozov, Gennady A. Morozov,
Ilnur I. Nureev and Anvar A. Talipov

Additional information is available at the end of the chapter

http://dx.doi.org/10.5772/59144

1. Introduction

The chapter is devoted to applications and construction principles of poly-harmonic (two-frequency or four-frequency) cw laser systems for characterization of different nonlinear scattering effects in fibers and reflection of devices based on fiber Bragg gratings (FBG) in telecommunication lines and sensor nets. In particular, we'll speak about evaluation of Mandelstam-Brillouin gain contour, Raman scattering contours and FBG reflection spectra characterization. Investigation methods and approaches are based on the unity of resonant structures of generated fiber responses on exciting and probing radiation or external physical fields for all given effects. The main decision is based on poly-harmonic probing of formed resonance responses.

At a certain level of the laser power, exciting the optical fiber, resonant contours of Mandelstam-Brillouin and Raman scattering are formed [1]. The first are based on periodic photon-phonon interactions, the second – the photon-photon ones. Similarly, spectral reflection characteristics of Bragg gratings, based on periodic variation of the refractive index in the fiber core, can be described by the resonant contour [2]. In telecommunication lines Mandelstam-Brillouin and Raman scatterings are undesirable effects, but in sensor nets there are the main sources of measuring information. FBG, as known, is the powerful instruments as for telecommunication lines and so on sensor nets design. Thus, characterization of Mandelstam-Brillouin gain and Raman scattering contours and FBG reflection spectra is the actual and important task for scientists and designers. The typical characteristics of given effects are discussed in the first part of the chapter.

To convert the information about the spectral contours characteristics are classically used broadband or tunable over a wide range optoelectronic means (optical spectrum analyzers, tunable lasers, optical reflectometers in time (OTDR) and frequency (OFDR) domains, scanning Fabry-Perot interferometers, diffraction gratings with CCD, and etc.) and complex "fit" algorithms for determining a desired value of accuracy of the central wavelength of the contours [3]. In recent years, significant progress in terms of accuracy and resolution of measurements, as well as practicality, was registered in the use of narrowband poly-harmonic technology [4] for characterization of contour spectrums that makes them competitive for the above mentioned methods in metrological characteristics, ease and cost of implementation. Their main advantage is that no measurements in the resonance region of spectral characteristics are necessary, that allows eliminating the influence of power instability of probing laser radiation and to detect information on the difference inter-harmonic frequency in the region with small noise level of photo-detector.

Second part of the chapter is devoted to poly-harmonic characterization of Mandelstam-Brillouin gain contours, Raman scattering contours and FBG reflection spectra for telecommunication applications. For example, Mandelstam-Brillouin frequency shift for silica fibers is about 10-20 GHz, and Mandelstam-Brillouin gain is observed in a bandwidth of 20-100 MHz [1]. The main parameters are the central frequency of a gain spectrum, its Q-factor and gain coefficient. The classical method for characterization of stimulated Mandelstam-Brillouin scattering (SMBS) gain spectrum is based on use of two lasers: one – for SMBS pumping, and another – for probing of generated gain spectrum [5]. The disadvantage of this method is need in strong control of a frequencies difference of two sources. Not long ago the measurement system which is free from this drawback was presented [6]. It is based on SMBS gain spectrum conversion from optical to the electrical field by single-sideband amplitude modulated radiation, in which the upper sideband is suppressed. Despite advantages, realization of this method is not always effective; because relevant low sensitivity of measurements is remained, similar to measurements by double-band amplitude modulated probing radiation in a wide bandwidth. A new method for SMBS gain spectrum characterization in single-mode optical fiber was presented in our papers [7-8]. It is based on use of advantages of single-sideband modulation and two-frequency probing radiation, which gives possibility of transfer the data signal's spectrum in the low noise region of a photo-detector. Also this radiation is characterized by effective procedure of received spectral information processing by the envelope's characteristics (phase and amplitude) of two spectral components beats. In the end of second part we also go back to the issues of poly-harmonic analysis of the FBG reflection spectra affected by us in [9-10].The modernization of previously used methods [4] will be presented, which based on the four-frequency probing radiation and only amplitude analysis of the envelopes [11]. Consideration of stimulated Raman scattering (SRS) in this part will be carried out only in general terms because of its negligible impact on the performance of telecommunication none-WDM lines [1].

Third part of the chapter is devoted to poly-harmonic characterization of Mandelstam-Brillouin gain contours, Raman scattering contours and FBG reflection spectra for sensor nets applications. An illustrative example of the relevance of considered issues is the use of all three

http://dx.doi.org/10.5772/59144

given physical mechanisms in distributed and the quasi-distributed sensor nets for down-hole telemetry [12,13]. If Mandelstam-Brillouin and Raman scatterings are carrying distributed information of the measured parameters (temperature, pressure), the FBG gratings allows to receive its point localization and flow velocity data [14,15]. For more information OTDR with Rayleigh scattering can be used and characterized to the Mandelstam-Brillouin ones by Landau-Placzek relation [16]. So way it seems reasonable to use a single radiation source for getting fiber-forming response to external stimuli, forming its special signal shape or spectra, optimized for recording spectrally separated responses from various nonlinear effects and reflections, and monitoring their bound to the central wavelength of the radiation. Some pair wise effects of such an implementation are known in practice of Weatherford, Schlumberger, Halliburton and other companies. Comprehensive option to generate and use of responses from the three types of scattering and reflection from the Bragg gratings not yet been studied. Its implementation could put information redundancy in the process of measuring, the use of which would improve the metrological characteristics systems being developed.

In fourth part perspective systems and their elements are presented, describing and discussing the methods, tools and systems parameters of means to get poly-harmonic radiation on the base of dual-drive MZM, scanning and poly-harmonic (more than four harmonics) methods for SMBS characterization based on technology transfer from LIDAR systems, designing of notch filters for blocking of elastic Rayleigh scattering in SRS and SMBS measurements. Additionally Raman and Mandelstam-Brillouin scattering in sensor nets so as a FBG reflection carry vast amount information about fiber conditions but sometime have low energy level. That's why it's one more cause to detect these types of scattering with high SNR and determine their properties. Applying of photo mixing allows significantly increase the reflectometeric system sensitivity under the condition of weak signals and receives information from frequency pushing of backscattered signal spectrum [56]. We offer in [4] to use two-frequency heterodyne and the second nonlinear receiver in the structure of reflectometers and now discuss its advantages comparatively to other methods of SNR increasing in the end of the fourth part.

In conclusion we'll resume results of above mentioned researches, mark it practical implementation and show new tasks in Mandelstam-Brillouin gain contours, Raman scattering contours and FBG reflection spectra characterization.

2. Spectral characteristics of SMBS gain, SRS scattering and FBG reflection contours

2.1. Spectral characteristics of SMBS gain and SRS scattering contours

Two important nonlinear effects in optical fibers, known as SRS and SMBS, are related to vibration excitation modes of silica and fall in the category of stimulated inelastic scattering in which the optical field transfers part of its energy to the nonlinear medium [1]. Even though SRS and SMBS are very similar in their origin, the main difference between the two is that

optical phonons participate in SRS while acoustic phonons participate in SMBS. In a simple quantum-mechanical picture applicable to both SRS and SMBS, a photon of the incident field (called the pump) is annihilated to create a photon at a lower frequency (belonging to the Stokes wave) and a phonon with the right energy and momentum, to conserve the energy and the momentum. Of course, a higher-energy photon at the so-called anti-Stokes frequency can also be created if a phonon of right energy and momentum is available. Different dispersion relations for acoustic and optical phonons lead to some basic differences between the two. The fundamental one is that SMBS in single-mode fibers occurs only in the backward direction whereas SRS can occur in both directions.

Both the Raman-gain spectrum $g_R(\nu)$ and the Mandelstam-Brillouin-gain spectrum $g_{MB}(\nu)$ have been measured experimentally for silica fibers. The Raman-gain spectrum is found to be very broad, extending up to 40 THz [17]. The peak gain $g_R \approx 6\times10^{-14}$ m/W at pump wavelength near 1.5 μm and occurs for a spectral shift of about 13.1 THz. In contrast, the Mandelstam-Brillouin-gain spectrum is extremely narrow and has a bandwidth of <100 MHz. The peak value of Mandelstam-Brillouin-gain occurs, for the Stokes shift of ~10 GHz, for pump wavelengths near 1.5 μm. The peak gain $g_{MB} \approx 6\times10^{-11}$ m/W for a narrow-bandwidth pump [18] and decreases by a factor of $\Delta\nu_P/\Delta\nu_{MB}$ for a broad-bandwidth pump, where $\Delta\nu_P$ is the pump bandwidth and $\Delta\nu_{MB}$ is the Mandelstam-Brillouin-gain bandwidth. As the Mandelstam-Brillouin-gain coefficient g_{MB} is larger by nearly three orders of magnitude compared with g_R, typical values of SMBS threshold are ~1 mW and for SRS threshold are ~1 W.

Although a complete description of SRS $g_R(\nu)$ in optical fibers is quite involved, the spectral characteristics for SMBS $g_{MB}(\nu)$ can be described by a simple relation. Little reminding – SMBS is a result of scattering of light on acoustic waves (acoustic phonons), that are excited by thermal fields and produce periodic modulation of the refractive index of fiber [1]. As a result of Bragg diffraction the induced grating of refractive index scatters the pumping radiation. As the scattered light undergoes a Doppler effect, the frequency shift ν_{MB}, caused by SMBS, depends on acoustic velocity and is given by

$$\nu_{MB} = \frac{2nV_A}{\lambda_P}, \tag{1}$$

where V_A acoustic velocity in the fiber, n refractive index, λ_P pump wavelength. The shape of the SMBS gain spectrum is determined by strong attenuation of sound waves in silica. Growth of Stokes wave's intensity is characterized by gain coefficient $g_{MB}(\nu)$, maximum at $\nu=\nu_{MB}$. Because of exponential decay of the acoustic waves, the gain spectrum $g_{MB}(\nu)$ will have the Lorentzian spectral profile

$$g_{MB}(\nu) = g_0 \frac{(\Delta\nu_{MB}/2)^2}{(\nu-\nu_{MB})^2 + (\Delta\nu_{MB}/2)^2}, \tag{2}$$

http://dx.doi.org/10.5772/59144

where $\Delta\nu_{MB}$ spectrum full width at half maximum. The maximum gain is given by

$$g_{MB}(\nu_{MB}) = g_0 = \frac{2\pi n^7 p_{12}^2}{c\lambda_P^2 \rho_0 V_A \Delta\nu_{MB}}, \tag{3}$$

where p_{12} longitudinal acousto-optic coefficient, ρ_0 density of material, c light speed in vacuum.

SMBS using allows to measure temperature (frequency shift of ν_{MB} about 1 MHz /°C) and strain (frequency shift of ν_{MB} about 493 MHz/%) of fiber so provide distributed technologies in sensor nets [1].

Let's return to the description of SRS $g_R(\nu)$ in optical fibers [1]. A weak Stokes signal launched into a fiber with a stronger pump will be amplified due to SRS as discussed in this chapter. The amplification of the signal is described through the following equation

$$g_R(\nu) = \sigma_0(\nu)\frac{\lambda_s^3}{c^2 \eta n^2(\nu)}, \tag{4}$$

where η is Planck's constant, λ_s is the Stokes wavelength, $n(v)$ is the refractive index, which is frequency dependent. The spontaneous Raman cross section $\sigma_0(\nu)$ is defined as the ratio [1] of radiated power at the Stokes wavelengths to the pump power at temperature 0 °K, which can be obtained with the measured Raman cross-section $\sigma_T(\nu)$ at temperature T °K, the thermal population factor $N(v, T)$ and Boltzmann constant κ_B:

$$\sigma_0(\nu) = \sigma_T(\nu) / \left(N(\Delta\nu, T) + 1\right), \tag{5}$$

$$N(\Delta\nu, T) = 1 \Big/ \exp\left(\frac{\eta c \Delta\nu}{\kappa_B T} - 1\right). \tag{6}$$

The $g_R(\nu)$ in (4) is the spontaneous Raman gain coefficient in bulk glass and is uniform in all directions. For the first time, the Gaussian decomposition technique was proposed earlier in [19] for a spontaneous Raman spectrum. It is known that the Raman gain profile differs from the spontaneous Raman spectrum, especially in the low frequency region [21]. So for SRS the Raman gain coefficient at the Stokes frequency $\nu_S = \nu_P - \nu$ with some assumptions can be written as follows [20]

$$g_R(\nu) \approx \frac{\nu \tilde{A}}{\left(\nu_S^2 - \nu^2\right)^2 + \nu^2 \tilde{A}^2}, \tag{7}$$

where ν_S and ν are the resonance and phonon angular frequencies, respectively, Γ is the phonon damping constant.

Model analysis of the Raman spectrum with Gaussian profiles is based on the following expression [21]:

$$g_R(\nu) = g_R \sum_{i=1}^{N_m} A_i \exp\left[-\left(\nu - \nu_{\nu,i}\right)^2 / \Gamma_i^2\right], \tag{8}$$

where N_m is the number of modes used for decomposition, υ,i is the central frequency of i-th Gaussian profile, $\Gamma_i = \mathrm{FWHM}_i / \left(2\sqrt{\ln 2}\right) \approx 0.6\ \mathrm{FWHM}_i$, where FWHM_i is the full width at the half maximum of i-th Gaussian profile. Amplitudes Γ_i together with υ,i and Γ_i are used as parameters in the nonlinear fitting procedure. There are two important aspects of the developed decomposition procedure. Firstly, this approach is seen as a possible method of subdividing the density of states according to specific contributions. Secondly, function $g_R(\nu)$ that gives the best fit of the experimental Raman gain profile is constructed [21]. We can see SMBS gain spectra and its parameters on the fig. 1,a with the results of Lorentzian fitting [22], so as SRS gain spectra on the fig. 1,b with the results of triangle (linear) and Gaussian (nonlinear) fitting [23]. For the last one we can mark that Gaussian fitting is more applicable and accurate for the central lobe of spectra [24].

2.2. Spectral characteristics of FBG reflection contours

FBG couple the fundamental mode of an optical fiber with the same mode propagating in the opposite direction. This means that radiation propagating in the fiber at a certain wavelength (9) is reflected from the grating completely or partially. Central or resonant frequency FBG λ_{BG} is defined by following expression [2]:

$$\lambda_{\mathrm{BG}} = 2 n_{\mathrm{eff}} \Lambda, \tag{9}$$

where n_{eff} is effective refraction factor of the basic mode, Λ is the period of its modulation.

The characteristics of this reflection depend on the grating parameters. It is possible to describe the envelope R of FBG reflection spectra defined by detunes δ as:

$$R = \sinh^2\left[\kappa L \sqrt{1 - (\delta/\kappa)^2}\right] \Big/ \left\{\cosh^2\left[\kappa L \sqrt{1 - (\delta/\kappa)^2}\right] - (\delta/\kappa)^2\right\} \approx \tanh\left[\kappa L \sqrt{1 - (\delta/\kappa)^2}\right], \tag{10}$$

http://dx.doi.org/10.5772/59144

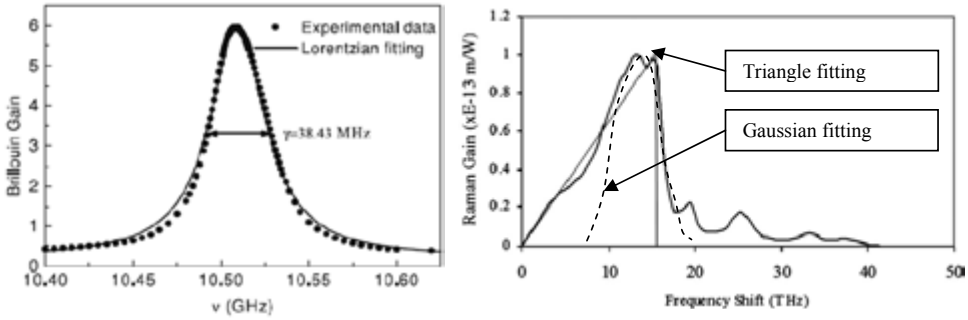

Figure 1. SMBS (a) and SRS (b) gain spectrums with the results of its fittings

Figure 1. SMBS (a) and SRS (b) gain spectrums with the results of its fittings

The characteristics of this reflection depend on the grating parameters. It is possible to describe the envelope R of FBG reflection spectra defined by detunes δ as:

where L – FBG length, κ – coupling factor of direct and return mode, (δ/κ) – relative detune.

Detune of FBG with period Λ is equal to $\delta=\Omega-(\pi/\Lambda)$, where $\Omega=2\pi n_{\text{eff}}/\lambda$ [2].

$$R=\sinh^2\left[\kappa L\sqrt{1-(\delta/\kappa)^2}\right]\Big/\left\{\cosh^2\left[\kappa L\sqrt{1-(\delta/\kappa)^2}\right]-(\delta/\kappa)^2\right\}\approx\tanh\left[\kappa L\sqrt{1-(\delta/\kappa)^2}\right], \quad (10)$$

The spectral width of the resonance of a homogeneous FBG (fig. 2,*a*) measured between the first zeroes of its reflection spectrum is described by the expression

where L – FBG length, κ – coupling factor of direct and return mode, (δ/κ) – relative detune. Detune of FBG with period Λ is equal to $\delta=\Omega-(\pi/\Lambda)$, where $\Omega=2\pi n_{\text{eff}}/\lambda$.

The spectral width of the resonance of a homogeneous FBG (fig. 2,*a*) measured between the first zeroes of its reflection spectrum is described by the expression

$$\Delta\lambda_{\text{BG},0}=2\lambda_{\text{BG}}\frac{\Lambda_{BG}}{L}\left[1+\left(\frac{\kappa L\sqrt{1-(\delta/\kappa)}}{\pi}\right)^2\right]^{1/2}. \quad (11)$$

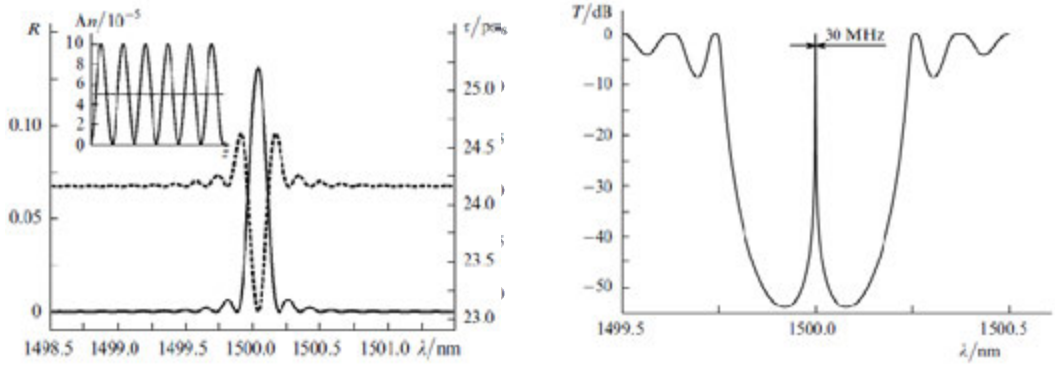

Figure 2. FBG reflection (a) and FBG-PS transmittance (b) calculated spectrums

The resonant FBG wavelength λ_{BG} depends on fiber temperature and from mechanical stretching or compressing pressure enclosed to it. This dependence is described by a following equation:

The resonant FBG wavelength λ_{BG} depends on fiber temperature and from mechanical stretching or compressing pressure enclosed to it. This dependence is described by a following equation:

$$\Delta\lambda_{\text{ВРБ}}=2n_{\text{эфф}}\Lambda\left(\left\{1-\left(\frac{\xi^2}{2}\right)\left[P_{12}-\nu(P_{11}+P_{12})\right]\right\}\varepsilon+\left[\frac{1}{\Lambda}\frac{\partial\Lambda}{\partial T}+\frac{1}{n}\frac{\partial n}{\partial T}\right]\Delta T\right), \quad (12)$$

where ΔT – temperature change, ε – the enclosed pressure, the second item composed in a figure brace reflects photo elasticity factor. This parity gives typical values of λ_{BG} shift depending on temperature ~0,01 nm/°K from relative lengthening of a fiber ~ $10^{-3}(\Delta L/L)$ (nm).

$$\Delta\lambda_{\text{ÂÐÁ}} = 2n_{\text{ýôô}}\Lambda\left(\left\{1-\left(\frac{\xi^2}{2}\right)\left[P_{12}-\nu\left(P_{11}+P_{12}\right)\right]\right\}\varepsilon+\left[\frac{1}{\Lambda}\frac{\partial\Lambda}{\partial T}+\frac{1}{n}\frac{\partial n}{\partial T}\right]\Delta T\right), \tag{12}$$

where ΔT is temperature change, ε is the enclosed pressure, the second item composed in a figure brace reflects photo elasticity factor. This parity gives typical values of λ_{BG} shift depending on temperature ~0,01 nm/°K from relative lengthening of a fiber ~ 10^3 $(\Delta L / L)$ (nm) [2].

The introduced phase shift (PS) [2] leads to the appearance of a narrow transmission band of width of a few tens of megahertz within the reflection band of FBG. Figure 2, b shows the calculated transmission spectrum of such FBG-PS grating. The phase shift in the grating can be introduced during the writing of the whole structure or later in the preliminary written grating. As the phase shift is increased (which is usually realized by writing two spatially separated gratings with the same FBG), the number of transmission regions in the reflection band increases, and such a structure is called, similarly to bulk optics, a Fabry-Perot interferometer (or filter). FBG-PS becomes the grate instrument in telecommunication and sensor nets [25-27].

The FBG reflective spectrum line shape can be approximated with a Gaussian profile [28]

$$R(\lambda) = R_B \exp\left[-4ln2\left[\left(\lambda - \lambda_B\right)/\Delta\lambda_B\right]^2\right]. \tag{13}$$

where λ is wavelength, λ_B is the center wavelength or peak wavelength of FBG, $\Delta\lambda_B$ is the full width at half maximum, and R_B is the maximum reflectivity.

As is known, the spectral dependence of the transmission band of FBG-PS has almost Lorentzian profile [2, 29]. If we assume that the spectral line width of the laser emission lines is negligibly small (~ several KHz), the spectral dependence of the transmission band of FBG-PS can be represented as follows:

$$T(\lambda) = \frac{T_B(\Delta\lambda_B/2)^2}{\left[(\lambda - \lambda_B)^2 + (\Delta\lambda_B/2)^2\right]}. \tag{14}$$

where T_B is maximum transmittance on λ_B.

2.3. Discussion of results

Basics for the use of poly-harmonic probing methods of spectral characteristics for resonant circuits of arbitrary shape were described by us in a number of papers [4,9-10]. It is noted that their effective use (maximum slope of the measurement conversion) is possible at the location of equal amplitude symmetrical components of the probe radiation on the FWHM of contour with average frequency at the central (resonant) wavelength. Based on this requirement, the synthesis of the poly-harmonic (two-or four-frequency) probe radiation desired characteristics was carried out. The example results are shown in Tab. 1.

http://dx.doi.org/10.5772/59144

Effect	Fitting contour	Central peak	Bandwidth	FWHM
SRS	Gaussian	13,1 THz	25-45 THz	10-10 THz
SMBS	Lorentzian	10-11 GHz	20-100 MHz	10-50 MHz
FBG	Gaussian	1550 nm	0,1-1 nm	0,05-0,5 nm
FBG-PS	Gaussian/ Lorentzian	1550 nm	0,1-1/0,005 nm	0,05-0,5 /0,002 nm

Table 1. Spectral characteristics of Mandelstam-Brillouin gain contours, Raman scattering contours and FBG reflection spectra

We have show in [30-33] that poly-harmonic probing radiation can be forming by external electro-optic modulation of narrowband one-frequency laser one. For general estimations of requirements for electro-optic modulators we assume that 1 nm in wavelength band is 120 GHz in frequency bandwidth. Thus, the operating frequency of modulators, we need, must be equal from 10-20 MHz to 20-40 THz. Provision of the lower limit for the FBG-PS study causes no problems. To investigate the SMBS and FBG contours a wide range of modulators with a frequency range up to 100 GHz spacing are existed in $LiNbO_3$, GaAs, InP realizations. Direct solutions to achieve 20-40 THz frequency does not exist today. The use of electro-optic modulators in the mode of frequency multiplication (in 12-16 times) is possible to obtain bandwidth in units of THz. However, given that we are interested in the scattering of the central part of the SRS spectrum allocated by a Gaussian filter, you can use a tunable laser to deliver carrier laser radiation to 13.1 THz. Thus, the implementation of methods for poly-harmonic probing of Mandelstam-Brillouin gain, Raman scattering and FBG reflection contours spectral characteristics looks quite feasible.

3. Characterization of SMBS gain and FBG reflection spectra in telecom applications

3.1. Characterization of SMBS gain spectra

Characterization of SMBS gain spectrum in single-mode optical fiber is necessary in a number of applications. These are: an assessment of the distortions brought by SMBS in information, transferred on fiber-optical lines [34], processing and conversion of optical carriers and microwave sub-carriers in communication networks such as «radio-over-fiber» [35], failure or measuring conversion of temperature on ONU in phonon microwave spectroscopy of optical fiber in PONs [36,37]. For silica fibers shift of Mandelstam-Brillouin frequency is about 10-20 GHz, and Mandelstam-Brillouin gain is observed in a bandwidth of 20-100 MHz [7].

The main parameters are the central frequency of a gain spectrum, its Q-factor and gain coefficient.

The classical method for characterization of Mandelstam-Brillouin gain spectrum (MBGS) is based on use of two lasers: one – for SMBS pumping, and another – for probing of generated gain spectrum [5]. The disadvantage of this method is need in strong control of a frequencies

difference of two sources. An advanced method gives the solution of this problem. The optical modulator generates the double-frequency signal. This signal is the sidebands of the pump laser, which are used then for probing [38]. But the disadvantage of this method is need in considering the input power in the gain spectrum and mechanisms of energy transfer between the pumping and probing components. The absence of these components can lead to saturation of contour and appearance of significant inaccuracies in characterization of MBGS. A certain progress in systems of characterization of MBGS was reached by generating the scanning double-band amplitude modulated probing radiation from pumping radiation [39]. However this method is characterized by the low sensitivity, caused by need of reception and processing of signals in a wide bandwidth (10-20 GHz), and also strong influence on measurement inaccuracy of the upper sideband existence. The solution of this problem also was in use of the double-frequency radiation generated unlike [38] for pumping radiation [40]. One frequency corresponded to pump frequency, and the second-to its Stokes component, thus frequency shifted absorption contour corresponded to Mandelstam-Brillouin gain spectrum. The absorption contour was used for suppression of the upper sideband. However, this system has a high complexity and need in strong control of positions of Stokes component and pump component, and also an absorption contour, especially when scanning of a probing signal within 20-100 MHz [7].

Not long ago the measurement system which is free from this drawback [6] was presented. It is based on MBGS conversion from optical to the electrical field by single-sideband amplitude modulated radiation, in which the upper sideband is suppressed. Despite advantages, realization of this method is not always effective; because relevant low sensitivity of measurements is remained, similar to measurements by double-band amplitude modulated probing radiation in a wide bandwidth. The new method for characterization of gain spectrum of SMBS in single-mode optical fiber is presented in this part. It is based on use of advantages of single-band modulation and double-frequency probing radiation, which gives possibility of transfer the data signal's spectrum in the low noise region of a photo-detector. Also this radiation is characterized by effective procedure of processing of received spectral information by envelope's characteristics of beats of two spectral components [7].

3.2. Two-frequency probing of MBGS

For conversion of the complex MBGS from optical to the electrical field the optical single-sideband modulation with scanning of frequency of a sideband component is used, including the information about the frequency shift and Q-factor of the SMBS gain spectrum. The measurement method offered by us is based on the double-frequency probing radiation of a MBGS, not on the single-frequency one. Experimental setup for measurements is shown on fig. 3 [7].

The optical signal from a 1550-nm laser diode with a bandwidth about 100 kHz is divided into two paths by a fiber-optic coupler. In the first path signal is modulated by an optical single-sideband modulator. Signal from the frequency combiner is applied to one of the modulator's inputs. The optical single-sideband modulator is based on a dual-drive Mach-Zehnder modulator design. The modulated signal is applied to the Fiber under test (FUT), where the

http://dx.doi.org/10.5772/59144

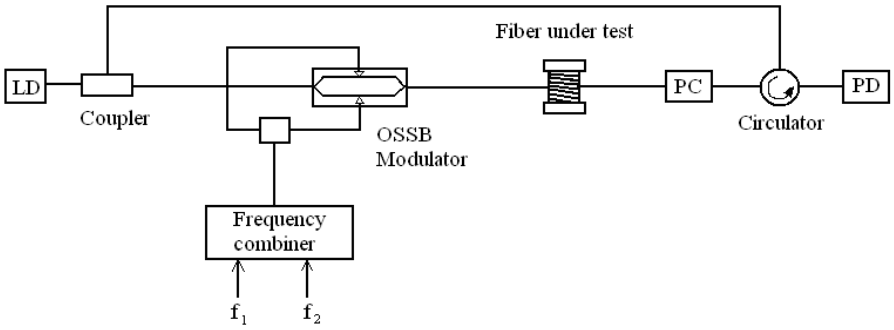

Figure 3. Experimental setup: LD – laser diode; PC – polarization controller; PD– photo-detector

optical radiation passed through the second path counter propagates. That non modulated radiation is the SMBS pump radiation in FUT [7].

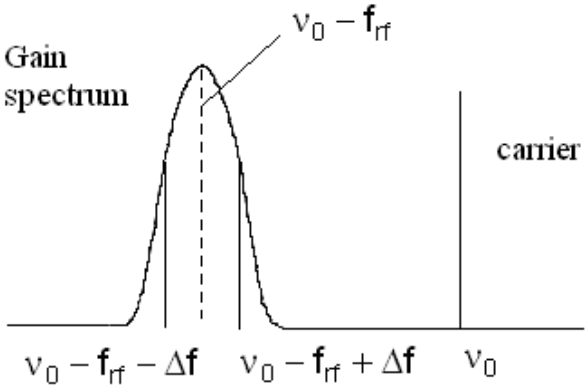

Figure 4. Probing of the gain spectrum by double-frequency signal

Thus, single-band double-frequency radiation with components $f_1 = f_{rf} - \Delta f$, $f_2 = f_{rf} + \Delta f$ probes the MBGS and the frequency $\nu_0 - f_{rf}$ tuned to the center of the gain spectrum conforms to its central frequency ν_{MB}, detuning Δf half of its FWHM, $\Delta\nu_{MB}$ and the carrier frequency ν_0 pump frequency $\nu_P = c/\lambda_P$. Double-frequency radiation, passed through the FUT, is received by photo-detector. Probing process is schematically shown in fig. 4 [57].

Radiation at the output of the optical single-sideband modulator is given by

$$E_{\text{in}}(t) = A_0 \exp(j2\pi\nu_o t) + \\ + A_{-1}\exp[\,\text{j}2\pi(\nu_0 - f_{rf} - \Delta f)t] + A_{-2}\exp[\,\text{j}2\pi(\nu_0 - f_{rf} + \Delta f)t], \quad (15)$$

where $A_0 = |A_0| \exp(j\varphi_0)$, $A_{-1} = |A_{-1}| \exp(j\varphi_{-1})$, $A_{-2} = |A_{-2}| \exp(j\varphi_{-2})$ complex amplitudes of the optical carrier and the double-frequency signal. This optical signal propagates through the FUT, which has an optical transfer function $H(\nu)$ characterizing the gain spectrum; therefore, the optical field at the output of the fiber is given by [57].

$$\begin{aligned} E_{out}(t) &= A_0 \left|H(\nu_0)\right| \exp\left[j \arg H(\nu_0)\right] \exp(j2\pi\nu_{0t}) + \\ &+ A_{-1} \left|H(\nu_0 - f_{rf} - \Delta f)\right| \exp\left[j \arg H(\nu_0 - f_{rf} - \Delta f)\right] \times \exp\left[j2\pi(\nu_0 - f_{rf} - \Delta f)t\right] + \\ &+ A_{-2} \left|H(\nu_0 - f_{rf} + \Delta f)\right| \exp\left[j \arg H(\nu_0 - f_{rf} + \Delta f)\right] \times \exp\left[j2\pi(\nu_0 - f_{rf} + \Delta f)t\right]. \end{aligned} \quad (16)$$

The output current on the beat frequency of the two probing components $2\Delta f$ is proportional to

$$\begin{aligned} |i_{\text{out}}(t)| \propto |A_{-1}||A_{-2}| &|H(\nu_0 - f_{rf} - \Delta f)||H(\nu_0 - f_{rf} + \Delta f)| \times \\ \times \cos[4\pi t \Delta \text{f} + \varphi_{-1} - \varphi_{-2} + \arg \text{H}(\nu_0 - f_{rf} - \Delta f) - \arg \text{H}(\nu_0 - f_{rf} + \Delta f)]. \end{aligned} \quad (17)$$

Analysis of (17) shows that, we can get the image of the optical transfer function at the frequencies of the two probing signals from the electrical output signal of the photo-detector. The optical transfer function of the FUT is equivalent to concatenation of the fiber linear transfer function and the MBGS [57].

3.3. Four-frequency characterization of the MBGS

As we mentioned above, the main parameters of the MBGS are the central frequency of a gain spectrum, its Q-factor and gain coefficient. It is significant that at the moment when center frequency of a double-frequency signal $\nu_0 - f_{rf}$ gets to the resonance frequency of a gain spectrum ν_{MB}, the envelope of the output signal is matched in phase with the envelope of the two-frequency signal at the FUT's input, and the modulation index of the output double-frequency signal's envelope is maximum and equal to 1 [57].

The measurement fractional inaccuracy of the central frequency can be 0,1% and determined by bandwidth of the laser radiation (in our case 0,1 MHz), and also by accuracy of keeping the difference frequency $2\Delta f$. Some part of the inaccuracy can be added by the appearance of not completely suppressed upper sideband of the double-frequency radiation in the spectrum. Among methods of its decreasing we can offer the usage of a chirp fiber Bragg grating, tuned on the suppression in the bandwidth of possible position change at scanning. We think that such solution is more effective, than offered in [40], as by efficiency of suppression, and also by ability to control the distortions, caused by chromatic dispersion [57].

http://dx.doi.org/10.5772/59144

Defining $\nu_0 - f_{rf} = \nu_{MB}$, we can find Q-factor of the MBGS. For this we offer the four-frequency method [58] or the method of the variation of difference frequency, which based on the dependence

$$Q_{1,2} = \frac{\nu_0 - f_{rf}}{f_1 - f_2} \sqrt{\frac{i_{\text{out}(\nu_0 - f_{rf})}}{i_{\text{out}1,2}} - 1}, \tag{18}$$

where $i_{\text{out}(\nu_0 - f_{rf})}$ and $i_{\text{out}1,2}$ amplitudes at center frequency and at components of the double-frequency signal at the output of the photo-detector when center frequency of the probing components at frequencies $f_1 = f_{rf} - \Delta f$ and $f_2 = f_{rf} + \Delta f$ is tuned on the center of gain spectrum. The value of $i_{\text{out}1,2}$ is determined by output signal of the photo-detector, and the value $i_{\text{out}(\nu_0 - f_{rf})}$ is unknown. If we change the Δf by a certain value $\Delta f'$, not changing the tuning on the center of gain spectrum, then we will get the new value of frequencies $f_3 = f_{rf} - \Delta f - \Delta f'$ and $f_4 = f_{rf} + \Delta f + \Delta f'$. For frequencies f_3 and f_4 we can rewrite the (18) as

$$Q_{3,4} = \frac{\nu_0 - f_{rf}}{f_3 - f_4} \sqrt{\frac{i_{\nu_0 - f_{rf}}}{i_{3,4}} - 1}. \tag{19}$$

Since $Q_{1,2} = Q_{3,4}$, from the combined solution of the equations (18) and (19) we get $i_{\text{out}(\nu_0 - f_{rf})}$ and then, inserting this value in one of the equations we find the Q-factor of the MBGS and half-width $\Delta\nu_{MB}$.

The advantage of the offered method is that in the measuring process the information signal is influenced by noises only of a bandwidth of the gain spectrum (20-100 MHz), not noises of all bandwidth from MBGS to the carrier (10-20 GHz). Therefore, SNR of the measurements in this case is 10^2-10^3 greater than similar ratio in previously offered methods. Inserting the known and determined by previously mentioned procedures frequency parameters ν_P, ν_{MB} and $\Delta\nu_{MB}$ in (3), we get the Mandelstam-Brillouin maximum gain coefficient value [7].

The presented method was tested in the laboratory of R&D Institute of Applied Electrodynamics, Photonics and Living Systems on the basis of coil of optical fiber Corning SMF-28 6 km long. At the pump power LDI-DFB 1550 5 mW, power of probing sideband components 90 nW we found the SMBS frequency shift is 10,54 GHz, gain coefficient – 20 dB, half-width – 36 MHz. The optical single-sideband modulator is based on a Mach-Zehnder JDS Uniphase OC-192 design. The oscilloscope Agilent InfiniiVision 7000, stabilized power supply PSS-1, the spectrum analyzer FTB 5240-S and the photodiode LSIPD-A75 were used [7].

So, a new method for characterization of gain spectrum of SMBS in single-mode optical fiber is presented. It is based on the usage of advantages of the scanning single-sideband modulation method and double-frequency probing method. For conversion of the complex SBS spectrum

from optical to the electrical field single-sideband modulation is used. Detection of double-frequency components position in the gain spectrum occurs through the amplitude modulation index of the envelope and the phase difference between envelopes of probing and passing components. The method is characterized by high resolution, SNR of the measurements increased of a two order, simplicity of the offered algorithms for finding the central frequency, Q-factor and Mandelstam-Brillouin maximum gain coefficient. Measurement algorithm is realized on simple and stable experimental setup. Among the methods of measurement inaccuracy decreasing, caused by not completely suppressed upper sideband of the double-frequency radiation, the usage of a chirp fiber Bragg grating, tuned on the suppression of it in the bandwidth of possible position change at scanning, can be considered [7].

3.4. Two-frequency characterization of FBG reflection spectra

FBG represents a longitudinal, periodic variation in the refractive index in the core of an optical fiber [2]. The main parameters of the grating are the distributions of the amplitude and period of the refractive index modulation, as well as the average value of the induced refractive index along the fiber axis. These parameters specify the spectral and dispersion parameters of gratings and, thus, determine their use in different applications of the fiber optics. FBG are widely used fiber lasers and amplifiers, in the fiber systems for measuring physical quantities, optical communication lines, and etc.

One of possible ways to decide specified problems of FBG reflection spectra characterization is based on FBG probing by the two-frequency radiation which average frequency at calibration point is adjusted on the central wavelength of FGB spectrum, and its detune and-or amplitudes difference between components are used as informative factors for definition of enclosed physical field parameter [4, 41]. The two-frequency measurement technique finds more and more appendices in various problems, for example: research of atmospheric gases absorption contours [42,43], measurement of dielectric coverings thickness [44], the analysis of FBG spectrum contour [45], an estimation of communication lines selective devices temperature drift [46], etc. Distinctions consist in parameters of used two-frequency signal or radiation, the requirements shown to their stability and techniques of measuring transformation.

In the given part we will use the two-frequency radiation received by Il'in-Morozov technique in Mach-Zender modulator [4], differing as high spectral cleanliness and stability at admissible change of formation parameters, and possibility of differential frequency simple tuning for use with various FBG characteristics. The specified generalized characteristics meet requirements to construction of probing radiations sources for fiber-optical nets [3]. As a technique of measuring transformation we will choose an integrated technique of the passed through or reflected from FBG two-frequency radiation envelope characteristics analysis.

At FBG contour shift caused by the application of physical fields, there is inequality $R_1 \neq R_2$ and restoration phase opposition of two-frequency radiation components. The kind of an inequality and a phase sign is defined by a direction of FBG contour shift, i.e. increase or reduction of the enclosed field parameter. The analysis of amplitudes and phases of the received components can be spent separately after their allocation by optical filters or time division in the

http://dx.doi.org/10.5772/59144

disperse environment; however these methods return us to problems of difficult spectral verification [47]. Therefore it was offered to spend processing of two-frequency radiation envelope [41].

Envelope amplitude U_R defined as:

$$U_R \approx \sqrt{R_1^2 + R_2^2 + 2R_1R_2\cos\left(k\Delta\delta t\right)}, \tag{20}$$

and an instant phase:

$$\phi_R \approx arctg\left\{\frac{\sin\left[\left(\phi_{R_2} - \phi_{R_1}\right) + k\Delta\delta t\right]}{R_1 / R_2 + \cos\left[\left(\phi_{R_2} - \phi_{R_1}\right) + k\Delta\delta t\right]}\right\}, \tag{21}$$

where ϕ_{R_1}, ϕ_{R_2} are accordingly the phases of output components R_1 and R_2.

For processing of the received values on amplitude we will enter modulation factor m:

$$m \approx \sqrt{1+\left(\delta_0 + \Delta\delta/2\right)^2} \Big/ \sqrt{1+\left(\delta_0 - \left(\Delta\delta/2\right)^2\right)}, \tag{22}$$

and on phase – we will find a difference of phases between envelopes of input and output radiations $\Delta\phi$ [41].

The example of the received measuring characteristics of the temperature FBG sensor on amplitude and a phase is presented accordingly on fig. 5,a and fig. 5,b. Analysis of the envelope 2 Δf parameters (22) and (21) made it possible to depict the measurement characteristics for determination of the central frequency of the gain spectrum by its amplitude (Fig. 5, *a*) and phase difference or sign of the phase difference (Fig. 5, *b*) between the envelopes at the FBG's input and output, similar to [48]. If the amplitude characteristic of measurements (fig. 5,*a*) has symmetric character, phase (fig. 5,*b*) allows resolving shift sign. Advantages of the amplitude characteristic are shown at operation in the field of "zero" detune parameter where there is an area of small signals for the phase characteristic [41].

For practical realization a setup shown in fig. 6 was assembled. Setup consists of the laser LDI-DFB 1550-20/50-T2-SM3-FA-CWP, calibration source Superlum SLD Pilot-4, the oscilloscope Agilent InfiniVision 7000, random waveform signal generator AFG3000, multimeter, MZM JDS Uniphase OC-192 Modulator, stabilized power supply PSS-1, the spectrum analyzer FTB 5240-S, an optical splitter, a circulator, FBG, the photodiodes LSIPD-A75 [59]. The spectra of two-frequency laser radiation is shown in Fig. 7, carried out in a

The example of the received measuring characteristics of the temperature FBG sensor on amplitude and a phase is presented accordingly on fig. 5,a and fig. 5,b. Analysis of the envelope $2\Delta f$ parameters (22) and (21) made it possible to depict the measurement characteristics for determination of the central frequency of the gain spectrum by its amplitude (Fig. 5, *a*) and phase difference or sign of the phase difference (Fig. 5, *b*) between the envelopes at the FBG's input and output, similar to [48]. If the amplitude characteristic of measurements (fig. 5,*a*) has symmetric character, phase (fig. 5,*b*) allows resolving shift sign. Advantages of the amplitude characteristic are shown at operation in the field of "zero" detune parameter where there is an area of small signals for the phase characteristic.

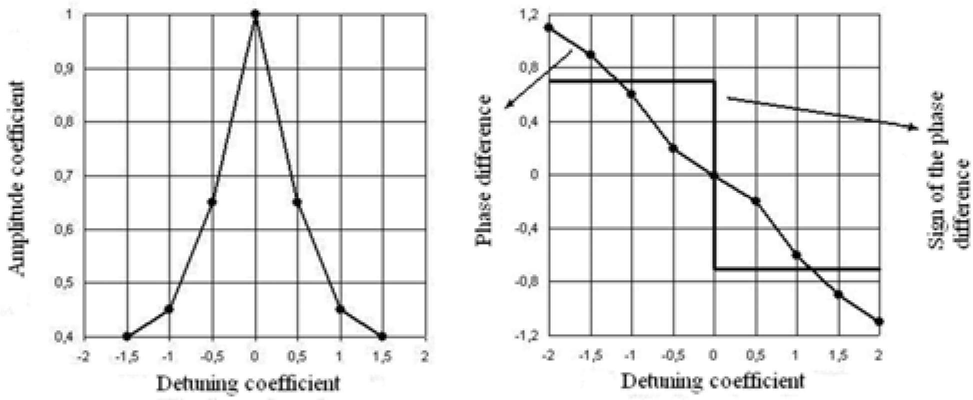

(a) (b)

Figure 5. Amplitude (a), phase difference and sign of the phase difference (b) between the envelopes at the FBG's input and output as a function of detuning and of the central frequency of the FBG

Figure 5. Amplitude (a), phase difference and sign of the phase difference (b) between the envelopes at the FBG's input and output as a function of detuning and of the central frequency of the FBG.

For practical realization setup shown in fig. 6 of assembled setup consists of the laser LDI-DFB 1550-20/50-T2-SM3-FA-CWP, calibration source Superlum SLD Pilot-4, the oscilloscope Agilent InfiniVision 7000, random waveform signal generator AFG3000, multimeter, MZM JDS Uniphase OC-192 Modulator, stabilized power supply PSS-1, the spectrum analyzer FTB 5240-S, an optical splitter, a circulator, FBG, the photodiodes LSIP-D-A70. The spectra of two-frequency laser radiation is shown in fig. 7, carried out in a Mach-Zehnder modulator by the Il'in-Morozov method for frequencies 2 GHz (fig. 7,*a*) and 8 GHz (fig. 7,*b*) at the output of FBG.

Mach-Zehnder modulator by the Il'in-Morozov method for frequencies 2 GHz (fig. 7,*a*) and 8 GHz (fig. 7,*b*) at the output of FBG [60].

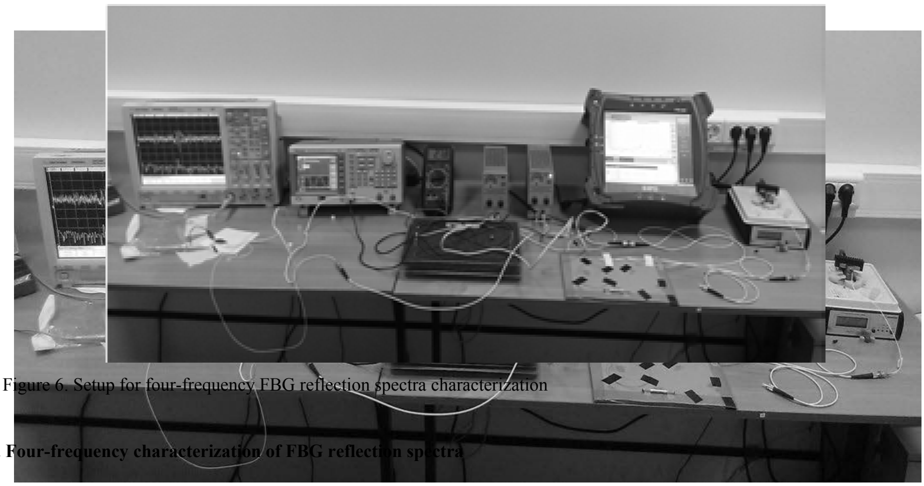

Figure 6. Setup for four-frequency FBG reflection spectra characterization

2.5. Four-frequency characterization of FBG reflection spectra

The analysis presented in [7] shows that from the electrical output signal we can get the image of the optical transfer function at the beat frequency of the two components of the probing signal, which will be determined by the change of their amplitudes and phases. At the moment when center frequency of a probing signal gets to the resonance frequency of a sensor (FBG) amplitudes and modules of the phases of both components are equal, the modulation index of the output signal's envelope is maximum and equal to 1, and the envelope of the signal is matched in phase with the envelope of the probing signal at the input.

Figure 6. Setup for four-frequency FBG reflection spectra characterization

3.5. Four-frequency characterization of FBG reflection spectra

The analysis presented in [7], [59] shows that from the electrical output signal we can get the image of the optical transfer function at the beat frequency of the two components of the probing signal, which will be determined by the change of their amplitudes and phases. At the moment when center frequency of a probing signal gets to the resonance frequency of a

http://dx.doi.org/10.5772/59144

sensor (FBG) amplitudes and modules of the phases of both components are equal, the modulation index of the output signal's envelope is maximum and equal to 1, and the envelope of the signal is matched in phase with the envelope of the probing signal at the input.

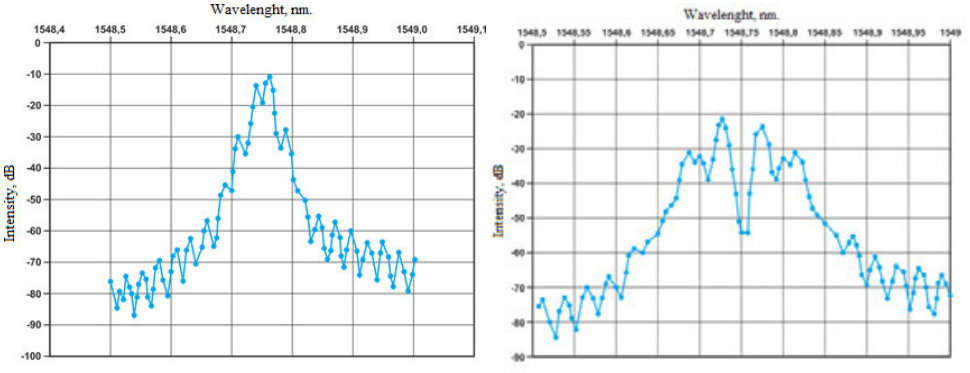

(a) (b)

Figure 7. The spectra of the two-frequency laser radiation at frequencies 2 GHz (a) and 8 GHz (b)

Figure 7. The spectra of the two-frequency laser radiation at frequencies 2 GHz (a) and 8 GHz (b)

When the two-frequency probing method is used the maximum measurement sensitivity is achieved by tuning its center frequency to the resonance frequency of a sensor (FBG), and the value of the detuning between the two components should be close to its band pass width at the half-maximum.

Inaccuracy of the measurements will depend on the correctness of maintaining the equality of the amplitudes and modules of the phases of probing signal's components, and on the signal/noise ratio of measurements. The phase measurements in the 30-100 GHz band are a complex task. Therefore, synthesis of poly-harmonic method that does not require processing of the phase information is an important problem. This method has been found and is a four-frequency method with two different average and difference frequencies. For reference, we note that in Section 2.3 we considered the four-frequency method with the overall average and different difference frequencies [7].

On fig.8 block diagram of device for precise four-frequency control method of FBG's resonant frequency is presented. In searching mode from driving generator of controller *10*, which is coupled with TFBG *3*, is coming retuning single frequency signal to the input of amplitude-phase four-frequency converter based on double port electro optic MZM.

Signal with frequency Ω, which corresponds the central peak half width of TFBG *3* or near it, is coming to the control input of amplitude-phase converter. Formed two two-frequency signals with two different average and difference frequencies is coming to the input of TFBG *3*. Output signal from TFBG *3* sends to the input of first and second photo-detectors *4*, *7*. Output four-frequency signal from TFBG *3* comes to the first and second selective filters *5*, *9*. Controller *10* receives information from first selective filter *5* about the frequency Ω1 and second selective

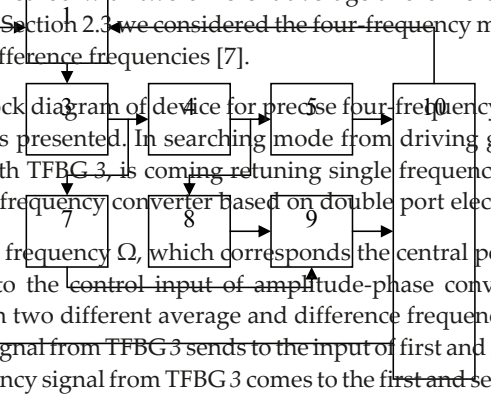

Figure 8. Device for precise four-frequency control method of FBG resonant frequency: 1 – four-frequency converter; 2 – DFB laser; 3 – FBG under test (TFBG); 4, 7 – first and second photo-detectors; 5, 9 – first and second selective filters; 6 – computer; 8 – amplifier; 10 – controller; 11 - interface

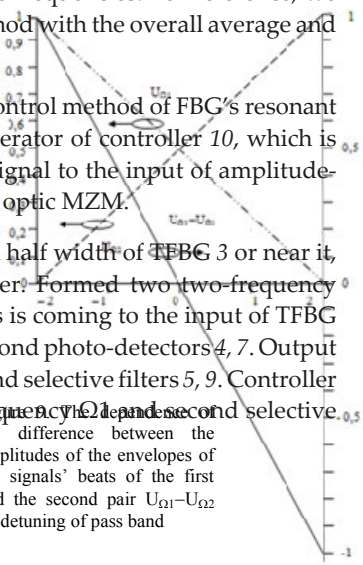

Figure 9. The dependence of the difference between the amplitudes of the envelopes of the signals' beats of the first and the second pair $U_{\Omega 1}-U_{\Omega 2}$ on detuning of pass band

frequencies. For reference, we note that in Section 2.3 we considered the four-frequency method with t different difference frequencies [7].

On fig.8 block diagram of device for precise four-frequency control method of FBG's resonant frequency is p made from tuning generator of controller *10*, which is coupled with TFBG *3*, is coming retuning single freque of amplitude-phase four-frequency converter based on double port electro optic MZM.

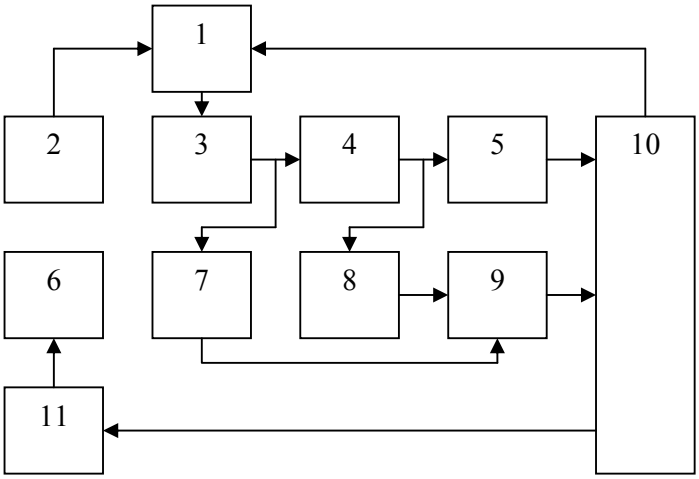

Figure 8. Device for precise four-frequency control method of FBG resonant frequency: 1 – four-frequency converter; 2 – DFB laser; 3 – FBG under test (TFBG); 4, 7 – first and second photo-detectors; 5, 9 – first and second selective filters; 6 – computer; 8 – amplifier; 10 – controller; 11 - interface

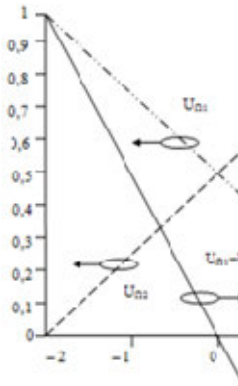

Figure 9. The dependence the difference between t amplitudes of the envelopes the signals' beats of the fi and the second pair $U_{\Omega1}$–U on detuning of pass band

Figure 8. Device for precise four-frequency control method of FBG resonant frequency: 1 – four-frequency converter; 2 – DFB laser; 3 – FBG under test (TFBG); 4, 7 – first and second photo-detectors; 5, 9 – first and second selective filters; 6 – computer; 8 – amplifier; 10 – controller; 11-interface

filter *9* on the frequency Ω2. Searching mode continuous till moment, when modu processing in controller detects $U_{\Omega1}U_{\Omega2}$=0. At the moment of resonance frequency output signal from controller *10* comes to the interface *11*, and computer *6* performs frequency measuring and begins to monitoring FBG spectra characteristics. Second photo-detector 7 and amplifier 8 are used for calibration between two two-frequency channels.

Fig. 9 shows the dependence of the amplitudes of the envelopes of the signals' beats of the first $U_{\Omega1}$ and the second $U_{\Omega2}$ pair, passed through FBG (left vertical axis), and their difference $U_{\Omega1}$-$U_{\Omega2}$ (right vertical axis) on detuning of FBG pass band (horizontal axis) for the case of supplying a signals with equal amplitude and center frequency matched with central frequency of pass band. Difference frequencies of the pairs Ω1 and Ω2 are not identical and are in the range up to 300 MHz. This allows the use of a narrow-band photo-detector [60].

In the generated pairs of signals passing through the FBG, amplitudes of the several components change according to the direction and value of frequency shift of pass band. When there is a frequency shift of FBG pass band depending on temperature changes, position of generated pair of signals' components with respect to the pass band will change, amplitudes of the envelopes of the pairs' beats will change and the differences between amplitudes of the envelopes of the first and second pairs' beats will change (passed through FBG according to presented dependence $U_{\Omega1}$-$U_{\Omega2}$). In this case, the measurements are taken at frequencies of envelopes, which are in a region of minimal noise of the photo-detectors [60].

Tests of the skilled device have been spent on FBG, made in FORC of the Russian Academy of Sciences (Moscow), calibrated in laboratories PGUTI (Samara), and have shown, that use of two-frequency probing FGB has allowed to reach errors of measurement of temperature 0,01 °C in a range 50 °C [41]. Thus the measurement error was defined basically by error of analogue

http://dx.doi.org/10.5772/59144

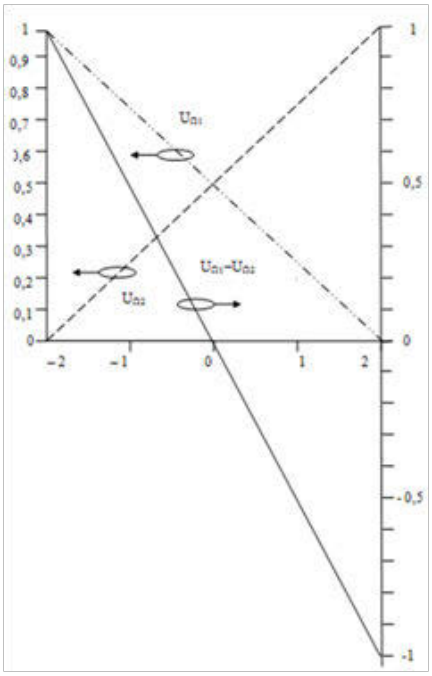

Figure 9. The dependence of the difference between the amplitudes of the envelopes of the signals' beats of the first and the second pair $U_{\Omega 1}U_{\Omega 2}$ on detuning of pass band

to digital coder of the controller *10* for the definition of temperature. The range of measured physical fields (temperature, pressure etc.) is defined by sensitivity of a grating to the measured parameter and value of differential frequencies of probing radiation, so in extreme points of frequency range displacement of a grating making radiations should not leave for level (0,05-0,1) R_0, where R_0 – factor of FGB reflection on the central frequency.

So, to reduce the measurement inaccuracy caused by phase fluctuations of system elements new poly-harmonic method was applied, based on a four-frequency narrow-band measurements without the use of phase analysis. The advantage of this approach is the ability of the measurement in a band up to 300 MHz with narrow-band low-noise photo-detector [59].

3.6. Discussion of results

This part of the chapter is devoted to poly-harmonic characterization of Mandelstam-Brillouin gain contour and FBG reflection spectra for telecommunication applications. Consideration of stimulated Raman scattering (SRS) in this part will be carried out only in general terms because of its negligible impact on the performance of telecommunication none-WDM lines [1]. We discussed the basics of MBGS and FBG spectrums characterization and proposed for the first time two new poly-harmonic methods. First is the four-frequency method with the overall average and different difference frequencies, discussed in section 2.3. Second is a four-

frequency method with two different average and difference frequencies, discussed in section 2.5. The advantage of both methods is the absence of the need to measure the phase characteristics of the tested contours. The results of its practical realization proved the results of mathematical modelling.

We call the first as “the method of difference frequency variation” analogically to the methods of frequency and capacity variations for Q-factor measuring. This method can be widely used in different systems for Q-factor measuring as in optical, so in microwave range. For example, in [49] we applied this method to monitoring of cure processes in composite materials. In optical range it can be applied to the measuring of Q-factor of transmitting window of CFBG with phase shift, for example presented in [23,50], which isn’t effected to shift of central wavelength. The second method with it simple realization can be widely used in precise sensor monitoring loops in laboratory conditions and special circuits for temperature control in the range of 5-10 °C with accuracy 0,01°C [11,51].

4. Poly-harmonic characterization of SMBS and SRS gain and FBG reflection spectra as the base of software defined down-hole telemetric systems

4.1. State-of-the-art in modern down-hole telemetric systems

In the last decade, fiber optic technologies (FOT) more intensively penetrate the oil and gas industry, especially in those interrelated topics in this industry as seismic, drilling, geophysical surveys in wells and oil and gas extraction. Different measuring system were developed based on FOT, which were characterized by high accuracy and better than electronic devices for the same purpose in terms of mechanical and thermal stability. Measuring elements (fiber or FBG) of such systems are not affected by magnetic and electric fields and are resistant to vibration and shock. Moreover, the measurements produced by the fiber optic wire line systems are not part of the wellbore which requires a power supply and operates only with the light sources.

Despite the fact that the installation of the pilot monitoring systems and production of oil wells, using FOT, began in 1980 and proved to be a number of positive factors, fiber telemetry means (FTM) installed today only in a small part of the hundreds of thousands of oil wells. On the one hand, this is due to the policy of preferential production of "easy" oil, on the other-a frequent haze fiber during hydrogen penetration into the ground and operating at high temperatures and pressures typical of oil production, and finally, the third one is the number of disadvantages of FTM structures themselves. Since stocks of "easy" oil is not unlimited, and emerging technologies allow to create a protected sealed fiber with the ability to work in the fields of temperatures up to 700 °C, the eyes of developers and operational organizations turned again to the possibility of installing FTM in wells by presenting to them the requirements to improve the metrological, feasibility, performance, which resulted in the appearance of the need for the optimization and upgrading of

http://dx.doi.org/10.5772/59144

the structural construction of complexes of the specified class. This shows the relevance of the theme of alleged applied research.

The fiber-optic distributed temperature sensor DTS based on SRS is the most common and is used in almost the entire world's oil companies. However, a number of shortcomings associated with the complexity of instrumentation, instability of pulse parameters, the need for complex calibration procedures, highlights the use of its concurrent methods based on SMBS and the methods used pure system on FBG. If the methods based on SMBS can achieve a spatial resolution of 0.1 m, the ones using FBG – 0.01 m.

Another important factor is the cost of FTM installing, which is for SRS equal to 50-100, SBS – 100-150, and FBG – 15-25 thousand of US dollars. It would seem the choice is clear, however, for the complexes at SRS and SMBS simply fiber as sensor is need, but for complexes on FBG it is necessary to "write" gratings in fiber and then to "pack" each of them in order to bring the properties of sensors for temperature, strain, pressure, acoustic noise measuring flow parameters. The FBG requires a significant investment in the pipeline sensor cable and makes it significant costs during the operational phase.

FTM based on FBG are widely used for the construction of point sensors, such as temperature control of the submersible pump and quazi-distributed temperature sensors. It is known their use in wells with temperatures up to 374 °C and pressures up to 220 bar, when cable length is up to 10 km and the error of measurement of pressure – up to 1%. FTM based on SMBS with the analysis in the time domain allow you to measure the temperature and pressure at the same time. The possibility of measuring the pressure reached with an accuracy of 2 , the temperature with an accuracy of 0.1 °C with a spatial resolution of 0,1 m, which is comparable with the characteristics of a wide class of FMT on FBG (1, 0,2 °C) at discrete installation respectively. Discrete setting of FBG is determined by the presence of inter-grating distortion when you install more than 5 arrays in series or a significant appreciation of the interrogator with an increase in the number of gratings.

In recent years, SRS FTM with the analysis in the frequency domain of the company LIOS Technology, GMBH are appeared on the market. These systems are the main competitors of the systems developed by the authors since 2004. The main advantages of said system are lower cost as compared with systems with time analysis, using a more stable cw-laser compared to pulse, the application of heterodyning circuitry for increasing the sensitivity of measurements and thereby improve the metrological characteristics. However, the work of these systems is provided only up to a temperature of 90 °C, at what rate, made by heterodyning, is realized in the secondary electron receiver, so the noise of the photo-detector continue to play a significant role in reducing the metrological characteristics of this FTM type. Transfer of the heterodyning in the optical range is accompanied by significant cost of the system through the use of additional Mach-Zehnder modulators (up to $ 1,000 per channel).

4.2. Background of software defined down-hole telemetric systems

Following conclusions about combined methods were made on the base of Weatherford, Schlumberger, Halliburton companies patent and development analysis:

- Halliburton use the system of wells monitoring on SMBS, the benefits of which are based on modern technological solutions in the field of measurement and application of the reference temperature sensors or pressure to separate multiplicative Brillouin sensor readings, such as, FBG;
- Schlumberger has patents with the use of FBG, which relate only to point measurements. Particularly noteworthy is the patent for an integrated system of down-hole thermometry that uses backscattered signal of one/any of the species: Rayleigh, Raman, Mandelstam-Brillouin scattering;
- the patent portfolio of Weatherford differs from a similar Schlumberger one by presence of a large number of FBG patents, which are using to some extent of complementary Raman and Mandelstam-Brillouin reflectometry, and are also used as point sensors. Particularly noteworthy is the patent for an integrated system of down-hole thermometry that uses backscattered signal of one /any of the species: Rayleigh, Raman, Mandelstam-Brillouin obtained for 7 years before such Schlumberger one.

In addition, it should be noted kinds of systems combined in pairs – Raman and Mandelstam-Brillouin, Raman and Rayleigh. We did not find projects that would take advantage of all three types of measurement procedures simultaneously. Modern technology, including patent solutions of our research group lead to the formation of parallel procedures in the fiber response of different nature (Raman, Mandelstam-Brillouin, Rayleigh and reflection from FBG) on the temperature and pressure in the well and make a universal procedure of poly-harmonic sensing responses, given their similar quasi-resonance character. These factors determine the urgency of developing a fiber optic down-hole telemetry system based on a combined non-linear reflectometry.

Scientific novelty of the research is to create a scientifically based methodological basis for the construction and implementation of technical and algorithmic solutions for down-hole fiber optic telemetry systems based on a combined nonlinear reflectometry, including methods and means for:

- formation of quasi-resonant nonlinear response (Raman scattering, Mandelstam-Brillouin scattering and reflection from FBG) in the fiber, carrying information about the distribution of temperatures and pressures;
- probing of Raman, Mandelstam-Brillouin and Bragg structures based on poly-harmonic radiation and quasi-coherent Rayleigh scattering poly-harmonic registration of temperature and pressure profiles;
- design of algorithms and software procedures for measuring the temperature and pressure, and flow rate of the liquid component composition, including the presence of occluded gas, based on the information obtained from the distributed and point sensors.

http://dx.doi.org/10.5772/59144

4.3. Planned research directions

Planned methods and approaches of down-hole fiber optic telemetry development based on the software-defined combined nonlinear reflectometry based on unity structures formed feedback from optical fiber to an external influence – temperature, pressure, flow parameters of the liquid (crude oil). If Mandelstam-Brillouin and Raman scatterings are carrying distributed information of the measured parameters (temperature, pressure), the FBG allows to receive its point localization and flow velocity data. For more information OTDR with Rayleigh scattering can be used and characterized to the Mandelstam-Brillouin ones by Landau-Plyachek relation. So way it seems reasonable to use a single radiation source for getting fiber-forming response to external stimuli, forming its special signal shape or spectra, optimized for recording spectrally separated responses from various nonlinear effects and reflections, and monitoring their bound to the central wavelength of the radiation. Some pair wise effects of such an implementation are known. Comprehensive option to generate and use of responses from the three types of scattering and reflection from the Bragg gratings not yet been studied. Its implementation could put information redundancy in the process of measuring, the use of which would improve the metrological characteristics systems being developed.

The second approach is based on the poly-harmonic probing and resonance response obtaining. In recent years, significant progress in terms of accuracy and resolution of measurements, as well as practicality, was registered in the use of narrowband poly-harmonic technology for characterization of contour spectrums that makes them competitive for the above mentioned methods in metrological characteristics, ease and cost of implementation. Their main advantage is that no measurements in the resonance region of spectral characteristics are necessary, that allows eliminating the influence of power instability of probing laser radiation and to detect information on the difference inter-harmonic frequency in the region with small noise level of photo-detector. The above-mentioned circumstances determine the relevance of the topic and the scientific and technological objectives to develop poly-harmonic methods and tools for the analysis of the spectral characteristics intended for separate registration of physical fields of different nature (temperature, pressure, flow parameters of the three-phase) and the construction on the basis of their optoelectronic down-hole telemetry using complex effects of nonlinear reflectometry in their software-defined domain.

The third approach concerns the structure of the construction of down-hole flow-meter. Over the past five years, down-hole monitoring systems installations are significantly increased. More than 90% are deep and complex branched wells. Traditionally, continuous monitoring is primarily used to control the pressure and temperature in the borehole. Thanks to the development and establishment of fiber optic down-hole flow-meters it became possible to measure the productivity of wells in its branches. Sophisticated flow structure defines the requirements for the construction of the flow-meter, however, note that its primary purpose is the definition of a flow within the wellbore, and not on the surface. To construct the flow set point is used temperature and acoustic pressure sensors. We have proposed to use for such purposes FBG-PS, FBG with a phase shift, which

is characterized by high resolution and the ability to check-in without a shift of the center wavelength, as shown in several studies [11,25,48,50].

4.4. Discussion of results

FOT systems and FTM for down-hole telemetry – a developing area of science and technology in Russia, which would create a competition international manufacturers of similar systems for the oil and gas industry and solve the problem of import substitution, significantly reduce the cost of the components used, displace traditional systems on electronic components. Based on the analysis of advanced domestic and foreign developments at the level of patents in the field of fiber optic systems of down-hole telemetry shows the relevance and scientific novelty of research areas, which determines the need to develop an integrated fiber optic down-hole telemetry system which is used to record the measured parameters for all kinds of scatterings assessments and distributed FBG – for point and the quasi ratings, including to resolve the multiplicative response to temperature and deformation (pressure) for FBG and Brillouin systems and error analysis in Raman systems. The studies will be established scientifically based methodological basis for building and technical and algorithmic solutions for the down-hole fiber optic telemetry systems based on a comprehensive nonlinear reflectometry and universal poly-harmonic probing of generated responses. These results allow to significantly improve the metrological characteristics of systems, including the reproducibility of results, because it will be used the measurement results with high redundancy on the basis of three or four feedback mechanisms of different nature of the optical fiber at the same environmental exposure. Scientific and methodological foundations and principles of systems can be used to monitor not only the down-hole structures, but any extended engineering structures and natural systems.

Proposed by us for the first time the concept, approaches and methods for its implementation allow reasonably formulate and solve the problem of creation of scientific and technical basis for designing software-defined down-hole fiber optic telemetry systems based on the combination of nonlinear reflectometry with improved metrological characteristics of poly-harmonic probing of sensing structures, including the removal of multiplicative and measurement errors caused by instability of the forming radiations in wide frequency range.

5. Elements of perspective reflectometeric systems with poly-harmonic probing

On the basis of two-frequency signal information structure investigation [4], [61], [62] with the purpose to find out main principles of combined interaction of its instantaneous values of amplitude, phase and frequency with arbitrary contour has been defined:

- instantaneous phase of two-frequency signal has a saw-tooth dependence. Speed of instantaneous phase changes is defined by components amplitude ratio. If $A_1/A_2=1$ the maximal speed of phase changing is observed. When two-frequency envelope has its minimum value, instantaneous phase has a shift, which depends on harmonic components

http://dx.doi.org/10.5772/59144

amplitude ratio. If the amplitudes of two-frequency signal components are equal, phase shift is equal to π ;

- it has been shown, that instantaneous frequency of two-frequency signal changes with deviation of it components amplitude ratio in range limited by signal frequencies. In case of components amplitude equality, instantaneous frequency coincides with average frequency of two-frequency signal $\omega_a=(\omega_1+\omega_2)/2$. When the envelope of two-frequency signal has its minimum value, frequency overriding occurs, which depends on harmonic components amplitudes ratio. When amplitudes of two-frequency components are equal, value of frequency overriding is infinity;
- modulation coefficient has a linear dependence on amplitudes ratio of two-frequency components. When amplitudes of frequency components are equal, modulation coefficient is maximal and equals unit value.

All obtained dependences can be used in symmetric poly-harmonic reflectometeric systems as informative and directive functions and in order to get information from selective optical fiber structures, like SRS, SMBS and FBG contours and so on [61], [62].

A joint analysis of given information allows us to determine the range of individual tasks that must be addressed when constructing symmetrical poly-harmonic reflectometeric systems. These tasks include following problems: integral self heterodyning ($A_0=0, A_1=A_2$); integral super heterodyning ($A_0>>A_1=A_2$); differential self heterodyning ($A_0=0, A_1\neq A_2$); differential super heterodyning ($A_0>>A_1\neq A_2$); receiving and processing frequency information ($\omega_0\neq(\omega_1+\omega_2)/2$) ; receiving and processing of phase information ($\phi_0\neq\phi_1=\phi_2$, $\phi_1\neq\phi_2$); receiving and processing the polarization ($A_0\perp A_1\| A_2$) and spatial information; information about instability ($A0\neq0$). Given the diversity of the set measuring tasks, their decisions, are presented further in this part of chapter, describing the methods, tools and systems parameters of means to get poly-harmonic radiation on the base of dual-drive MZM, scanning and poly-harmonic (more than four harmonics) methods for SMBS characterization, designing of notch filters for blocking of elastic Rayleigh scattering in SRS and SMBS measurements [61], [62].

Additionally Raman and Mandelstam-Brillouin scattering in sensor nets so as a FBG reflection carry vast amount information about fiber conditions but sometime have low energy level. That's why it's one more cause to detect these types of scattering with high SNR and determine their properties. Applying of photo mixing allows significantly increase the reflectometeric system sensitivity under the condition of weak signals and receives information from frequency pushing of backscattered signal spectrum. We offered previously to use two-frequency heterodyne and the second nonlinear receiver in the structure of reflectometers and discuss these questions in [4] [56].

5.1. Numerical simulation of poly-harmonic conversion in dual-drive Mach-Zehnder modulator

The numerical simulation in dual-drive Mach-Zehnder modulator [31,52] was carried out for signals with following parameters: amplitude of RF modulating signals was equal $V_1=V_2=V_\pi$;

MZM, scanning and poly-harmonic (more than four harmonics) methods for SMBS characterization, designing of notch filters for blocking of elastic Rayleigh scattering in SRS and SMBS measurements.

Additionally Raman and Mandelstam-Brillouin scattering in sensor nets so as a FBG reflection carry vast amount information about fiber conditions but sometimes have low energy level. That's why it's one more task to detect these types of scattering with high SNR and determine their properties. Applying of photo mixing allows significantly increase the reflectometeric system sensitivity under the condition of weak signals and receives information from frequency pushing of backscattered signal spectrum. We offered previously to use two-frequency heterodyne and the second nonlinear receiver in the structure of reflectometers and discuss these questions in [4].

4.1. Numerical simulation of poly-harmonic conversion in dual-drive Mach-Zehnder modulator

The numerical simulation in dual-drive Mach-Zehnder modulator [31,52] was carried out for signals with following parameters: amplitude of RF modulating signals was equal $V_1 = V_2 = V_\pi$; DC bias voltage applied to arm one and two was $V_{bias\ 1} = U_\pi/2$ and $V_{bias\ 2} = 3U_\pi/2$, respectively; phase difference between RF signals of two arms was changing. Resulted spectrums of output MZM signal for different phase difference between RF signals of two arms are presented on fig. 10-14.

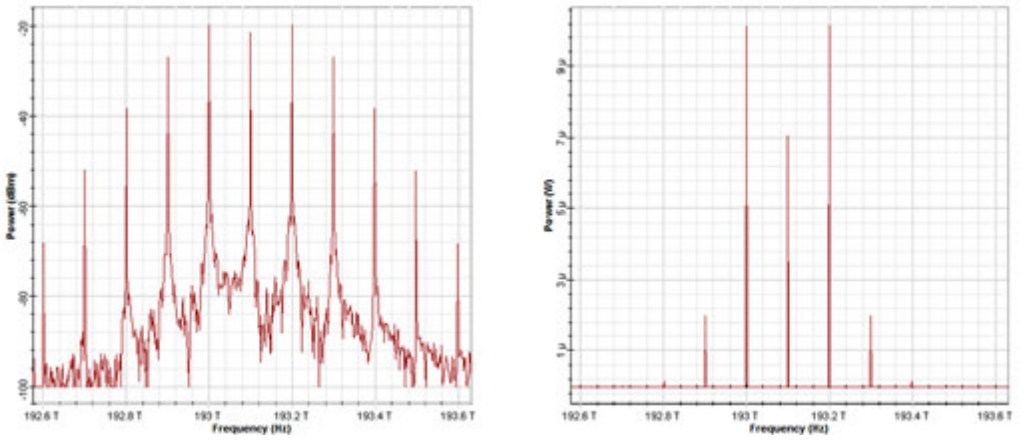

(a) (b)

Figure 10. MZM output signal spectrum for the case of $\Delta\psi = 0°$ (*a* – dBm, *b* – W)

Figure 10. MZM output signal spectrum for the case of $\Delta\psi=0°$ (*a* – dBm, *b* – W)

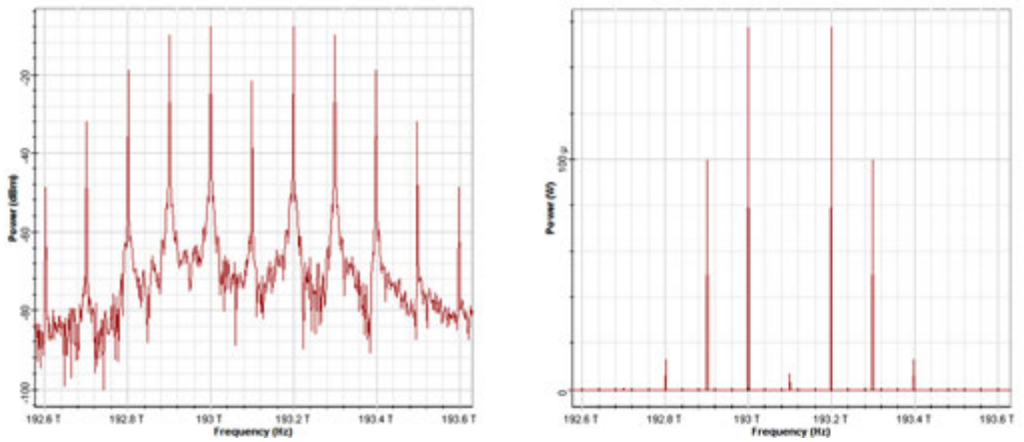

(a) (b)

Figure 11. MZM output signal spectrum for the case of $\Delta\psi = 45°$ (*a* – dBm, *b* – W)

Figure 11. MZM output signal spectrum for the case of $\Delta\psi=45°$ (*a* – dBm, *b* – W)

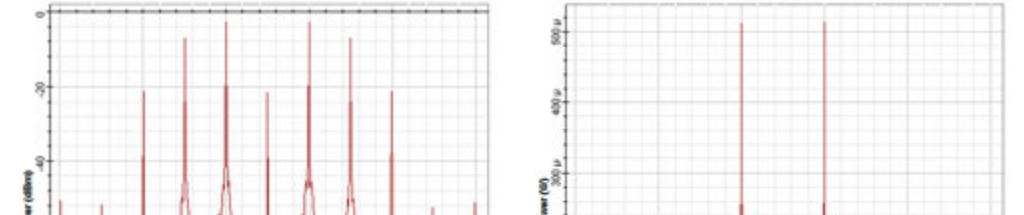

http://dx.doi.org/10.5772/59144

Figure 11. ° (*a* –

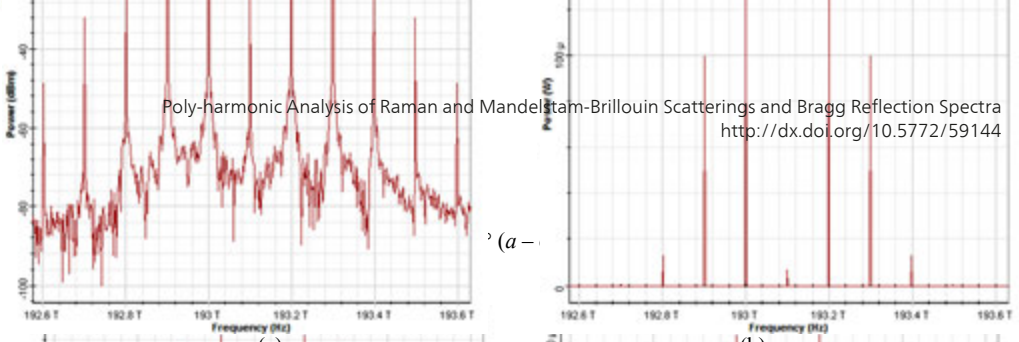

(a) (b)

Figure 11. MZM output signal spectrum for the case of Δψ = 45° (*a* – dBm, *b* – W)

Figure 12. M *a* –

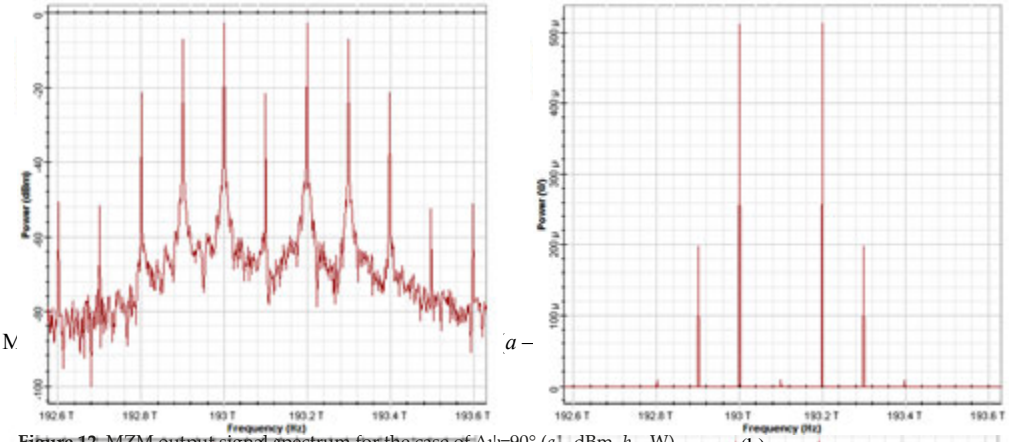

Figure 12. MZM output signal spectrum for the case of Δψ=90° (*a* – dBm, *b* – W)

(a) (b)

Figure 12. MZM output signal spectrum for the case of Δψ = 90° (*a* – dBm, *b* – W)

Figure 13. M ° (*a*

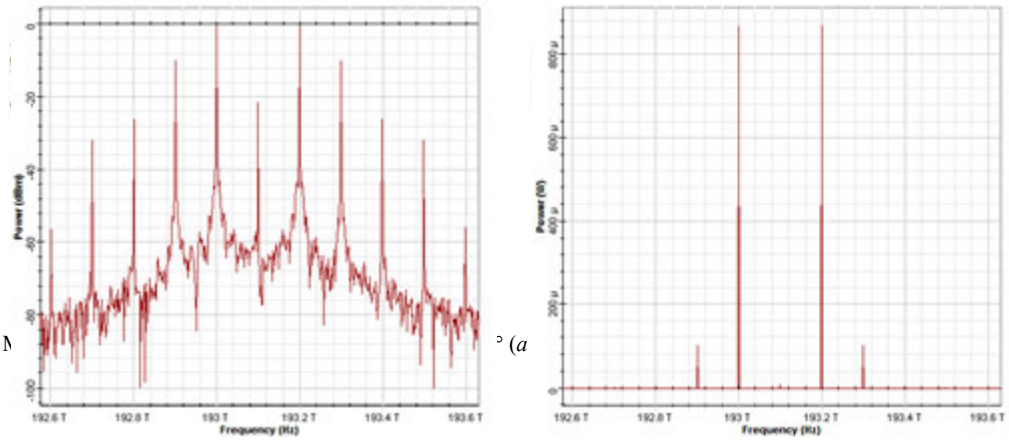

(a) (b)

Figure 13. MZM output signal spectrum for the case of Δψ = 135° (*a* – dBm, *b* – W)

Figure 13. MZM output signal spectrum for the case of Δψ=135° (*a* – dBm, *b* – W)

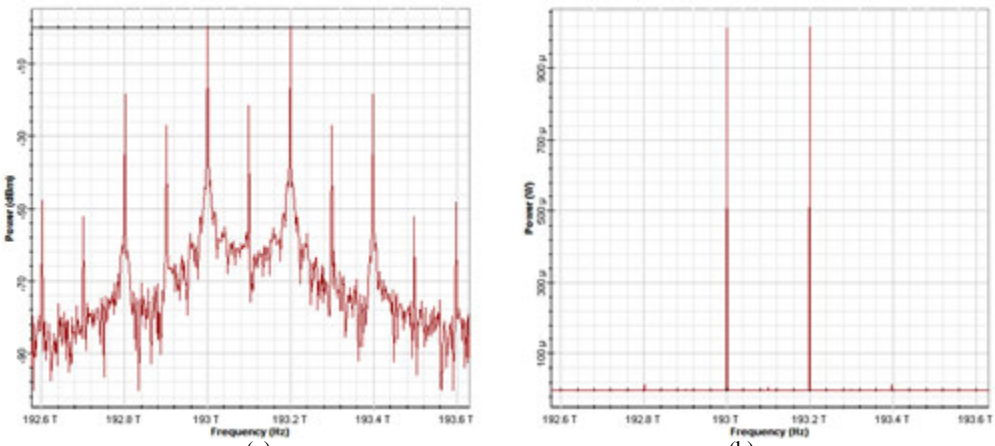

(a) (b)

Figure 14. MZM output signal spectrum for the case of $\Delta\psi = 180°$ (*a* – dBm, *b* – W)

Figure 14. MZM output signal spectrum for the case of $\Delta\psi=180°$ (*a* – dBm, *b* – W)

Signal, containing only two spectral components, was obtained for a case of phase difference $\Delta\psi = 180°$. The career and the other side components were suppressed more than 20 dB. Signals containing four spectral components, were obtained for a cases of phase difference $\Delta\psi=45°$ and $\Delta\psi=90°$. In order to get four-frequency signal with equal components differential regime of dual-drive Mach-Zehnder modulator has to be used. But in this case problem of not full suppression of initial carrier (one-frequency) radiation may arise. Utilization of notch filter for purpose of carrier suppression will be discussed in 4.5.

Signal, containing only two spectral components, was obtained for a case of phase difference $\Delta\psi = 180°$. The career and the other side components were suppressed more than 20 dB. Signals containing four spectral components, were obtained for a cases of phase difference $\Delta\psi=45°$ and $\Delta\psi=90°$. In order to get four-frequency signal with equal components differential regime of dual-drive Mach-Zehnder modulator has to be used. But in this case problem of not full suppression of initial carrier (one-frequency) radiation may arise. Utilization of notch filter for purpose of carrier suppression will be discussed in 4.5.

4.2. Two-frequency scanning for SMBS gain spectra characterization

The questions of interaction between scanning two-frequency probing radiation and SMBS gain spectra are considered. If the laser wavelength is modulated by the frequency:

$$\nu(t) = \nu_0 + \Delta\nu\cos\Omega t, \tag{23}$$

5.2. Two-frequency scanning for SMBS gain spectra characterization

where ν_0 is initial laser frequency, $\Delta\nu$ is modulation rate, than the intensity of SMBS gain spectra signal will could define from the equation:

The questions of interaction between scanning two-frequency probing radiation and SMBS gain spectra are considered. If the laser wavelength is modulated by the frequency:

$$I(t) = I_0 T(\nu_0) + I_0 T^{(1)}(\nu_0)\Delta\nu\cos\Omega t - 0{,}25 I_0 T^{(2)}(\nu_0)\Delta\nu^2\cos 2\Omega t + ..., \tag{24}$$

$$\nu(t) = \nu_0 + \Delta\nu\cos\Omega t, \tag{23}$$

where $T(\nu_0), T^{(1)}(\nu_0), T^{(2)}(\nu_0)$ are SMBS gain spectra transmittance (the reverse value of reflection) and its derivative by ν, correspondingly, I_0 is source intensity. Selective amplifier, which is tuned to the frequency Ω or 2Ω, allowed signal recovering from SMBS GAIN SPECTRA even with low gain and eliminate high level constant component $I_0 T(\nu_0)$ of the signal.

where ν_0 is initial laser frequency, $\Delta\nu$ is modulation rate, than the intensity of SMBS gain spectra signal will could define from the equation:

Frequency modulation allows sensitivity increasing of spectral photometric method at least in two orders with good SNR. Spectral resolution for derivative method is defined by frequency modulation rate $\Delta\nu$. Time resolution defines by modulation frequency Ω. Spectrum recovering accurate to constant component is accomplished by sequential signal integration.

$$I(t) = I_0 T(\nu_0) + I_0 T^{(1)}(\nu_0)\Delta\nu\cos\Omega t - 0{,}25 I_0 T^{(2)}(\nu_0)\Delta\nu^2\cos 2\Omega t + ..., \tag{24}$$

During two-frequency probing SMBS gain spectra is exploring by two signals with central frequencies $\nu_0 - \nu_T$ and $\nu_0 + \nu_T$. When $\nu_T = \Delta\nu/2$ where $T(\nu_0), T^{(1)}(\nu_0), T^{(2)}(\nu_0)$ are SMBS gain spectra transmittance (the reverse value of reflection) and its derivative by , correspondingly, I_0 is source intensity. Selective amplifier, which is tuned to the frequency Ω or 2Ω allowed signal recovering from SMBS GAIN modulation ν_0 sweeping frequencies is defined by:

$$\nu_1(t) = \nu_0 - \frac{\Delta\nu}{2}\left(1 + \cos\left(\Omega_0 t + \frac{\pi}{2}\right)\right),\quad \nu_2(t) = \nu_0 + \frac{\Delta\nu}{2}\left(1 + \cos\left(\Omega_0 t + \frac{\pi}{2}\right)\right). \tag{25}$$

Interaction between frequency modulated laser radiation and SMBS gain spectra causes power amplitude modulation (AM) of receiving signal. Modulation rate of such signal is straight to *Q*-factor, and AM envelope follows linear-frequency modulation (LFM). When central laser wavelength is tuned to central peak of SMBS gain spectra and frequency deviation equals spectrum half width, initial frequency of amplitude modulation is Ω_0, and its frequency deviation is $2\Delta\Omega$.

In work has been held modeling of signals processing for such system for direct and coherent detection. Usually in frequency ranging

http://dx.doi.org/10.5772/59144

SPECTRA even with low gain and eliminate high level constant component $I_0T(\nu_0)$ of the signal [10].

Frequency modulation allows sensitivity increasing of spectral photometric method at least in two orders with good SNR. Spectral resolution for derivative method is defined by frequency modulation rate Δν. Time resolution defines by modulation frequency Ω. Spectrum recovering accurate within constant component is accomplished by sequenced signal integration [8].

During two-frequency probing SMBS gain spectra is exploring by two signals with central frequencies $\nu_0-\nu_T$ and $\nu_0+\nu_T$. When $\nu_T=\Delta\nu/2$ modulation of sweeping frequencies is defined by:

$$\nu_1(t)=\nu_0-\frac{\Delta\nu}{2}\left(1+\cos\left(\Omega_0 t+\frac{\beta t^2}{2}\right)\right),\nu_2(t)=\nu_0+\frac{\Delta\nu}{2}\left(1+\cos\left(\Omega_0 t+\frac{\beta t^2}{2}\right)\right). \quad (25)$$

Interaction between frequency modulated laser radiation and SMBS gain spectra causes power amplitude modulation (AM) of receiving signal. Modulation rate of such signal is straight to *Q*-factor, and AM envelope follows linear-frequency modulation (LFM). When central laser wavelength is tuned to central peak of SMBS gain spectra and frequency deviation equals spectrum half width, initial frequency of amplitude modulation is Ω_0, and its frequency deviation is 2ΔΩ [10].

In work has been held modeling of signals processing for such system for direct and coherent detection. Usually in frequency ranging for extraction low frequency signal of telemetric frequencies which carries information of SMBS gain spectra properties within analyzing distance *R* in reception path received signal mixes with reference signal. In all cases measurement of subcarrier frequency increment $\Delta\Omega_R=2\beta R/c$ is performed by means of registration diversity between subcarrier frequencies of transmitted and received signals. Simulation has shown that under matching the demands for scanning SMBS gain spectra and LFM chirp resolution of spatial measurements, more strict conditions are applied by SMBS gain spectra properties. That causes decrease of spatial resolution. In case of direct detection of double frequency reflected signal auto heterodyning is performed with spatial coincidence of mixing rays. In that case signal spectrum transfers to the zone with low noise level of photo detector. Range control is performed by measurement the reduplicated frequency changes of modulating LFM chirp signal, and output signal frequency from intermediate amplifier of receiving system. SMBS gain spectra parameters control is performed by measurement of signal power level at that frequency. For short fibers, which require bands of receiving paths in the range 20-100 MHz, sensitivity increasing may total two orders [8].

In some works has been shown the possibility of using additional signals, which were none selectively influenced by testing SMBS gain spectra for increasing metrological properties of a system. In case of two-frequency source frequency modulation could be accomplished by two signals. The first confirms the demands for SMBS gain spectra scanning and LFM chirping, the second represents modulating signal with constant frequency within the limits of SMBS

gain spectra with amplitude two orders less than the scanning signal amplitude. In that case measuring signal will contain two items. The first $U_1 \approx k_1 f(I_0, T, R)\phi(\tau)$ depends on SMBS gain spectra optical properties, gauging equipment parameters and etc. The second item U_2, mostly is not under the influence of SMBS gain spectra, only from component $k_2 f(I_0, T, R)$. After normalization U_1 regarding U_2 for distance R (simultaneous signal selection) and assuming that k_1=k_2, we will get equation, which depends only on SMBS gain spectra properties $\phi(\tau)$.

Thus, two-frequency SMBS gain spectra scanning allows system increasing performance both in direct detection mode and normalizing mode, because reference signal parameters are determined and are not the signals of spurious modulation [8].

5.3. Multiple frequencies probing for SMBS gain spectra characterization

Analysis has shown that the main demand for SMBS gain spectra high precision measurements is high synchronization of phase, frequency, amplitude and polarization of probe signals. Sometimes it is impossible to fulfill those conditions even with the use of digital frequency synthesizer and locked-in lasers. Therefore the task of getting two-frequency and two-band oscillations with multiple frequencies and high synchronization is of current importance. Let us consider such method based on amplitude-phase conversion (Il'in-Morozov's method [4]).

Method is based on phase commutation by 180° of amplitude modulated signal at the moment when its envelope has minimum value. The basic task of research is defining the form and parameters of modulating signal $S(t)$ to receive an output two-frequency oscillation with suppressed carrier frequency ω_0. Total suppression of side components with $n \geq 3$ could be achieved with the use amplitude modulating oscillation $S(t)=S_0|\sin\Omega t|$. Than the resulting signal with amplitude modulation index b would have the following spectrum [8]:

$$e(t) = \frac{2E_0}{\pi}(1-b)\sum_n \frac{1}{n}\left\{\cos(\omega_0 + n\Omega)t - \cos(\omega_0 - n\Omega)t\right\} + \frac{\pi E_0 b}{4}\left\{\cos(\omega_0 + \Omega)t - \cos(\omega_0 - \Omega)t\right\}. \quad (26)$$

Amplitude of spectral components will be defined by Fourier series indexes, and for n=1 E_1=[$2E_0/\pi$][1b]+[$\pi E_0 b/4$], for $n \geq 3$ E_n=[$2E_0/\pi n$][1b]. When b_{opt}=1 spectrum contains two useful components with frequencies $\omega_0 \pm \Omega$, and the spurious products are suppressed. When the modulation index varies between (0,7-1)b_{opt} output signal nonlinear-distortions coefficient would be less than 1%.

Modulation signals given previously could be used for forming symmetric double band spectrum for multi frequency measurement systems. To realize them it is essential to solve equations set (25) for indexes, varying not only amplitude modulation index but also the value of phase commutation θ. Using the oscillation $S(t)=S_0|\sin\Omega t|$ we will get the following equations for amplitudes of spectral components [8]:

$$E_0 = \frac{E}{2}(1+\cos\theta); E_1 = E\left(\frac{1-b}{\pi} + \frac{\pi b}{8}\right)(1-\cos\theta); \quad (27)$$

http://dx.doi.org/10.5772/59144

$$E_n = \frac{E(1-\cos\theta)}{\pi n}(1-b) \text{ for n=3, 5, 7...; } E_n = \frac{bE(1+\cos\theta)}{1-n^2} \text{ for n=2, 4, 6 } \ldots \quad (28)$$

Equations (26) (27) allows to define spectral distribution of resulting signal with any b and θ. However, from point of view of simple technical realization we should look for forming oscillations without phase commutation using synthesis of oscillations with complex harmonic composition with k components, for example [8]:

$$S(t) = \sum_{k=1}^{\infty} S_k \cos\ (2k\ \Omega\ t + \pi), E_n = \frac{2E}{\pi}\left[\frac{1}{n} - \sum_{k=1}^{\infty}\frac{mk}{2}\left(\frac{1}{n+2k} + \frac{1}{n-2k}\right)\right], \quad (29)$$

where S_k are the partial amplitudes, E_n are the equations for Fourier indexes of its spectrum, m_k are partial indexes of amplitude modulation. Such approach of looking for forming oscillations will also allowed to take into account influence of real devices modulation characteristics nonlinearities on spectral distribution of output radiation, which are used to realize amplitude-phase conversion.

Differential frequency of two-frequency oscillation (25) when b_{opt}=1 is defined by frequency Ω of phase commutation θ. Its stability unambiguously concerned with frequency stability of driving voltages and instabilities of commutations devices. Really achievable value of differential frequency's instability with thermo-stating of driving generators is 10^8. During differential frequency's retuning, which is required in some types of measurements and rather simple realized with the use of amplitude phase conversion, minimum frequency shift is determined by modulators gain slope, and maximum frequency shift is determined by higher cutoff frequency of modulator and correlation between modulator and modulated frequencies [8].

Energy equality of side lobes and the effectiveness of their conversion are of great importance in multiple frequencies systems. Using the derived equations for the spectrums of output oscillations and taking into consideration properties of amplitude-phase conversion, i.e. using the additional power of amplitude modulation and phase commutation for forming the side lobes, we could determine, that power of the last one is nearly 60% of initial single frequency oscillation, and conversion index equals unit value without taking into account the loss in real modulators. Moreover multi frequency radiation allows any pair of formed frequencies using for differential analysis without retuning central laser frequency [8].

As it has been mentioned above retuning both laser frequency and difference frequency between spectral components either is very complex or is carried out nonlinearly. Simple way of SMBS gain spectra analysis could be realized with its multiple frequencies probing (fig.15).

If initial SMBS gain spectra probing by two-frequency signal with components A_1 and A_2 did not allowed the measurement of the central wavelength of SMBS gain spectra we should change the conditions of amplitude phase forming of probe signal. Solving the equation (25) with E_3=0 and limiting to four components we will get multiple frequencies signal with A_1, A_2,

A_5 and A_6. At that components A_1, A_2, A_5 lie on the left slope and component A_6 lies on the right. It could be defined from phase characteristics. As far as $A_2>A_6$ what is evident from envelope analysis of that pair cutout by band pass filter we should change the parameters of amplitude phase conversion of probe signal one more time [10].

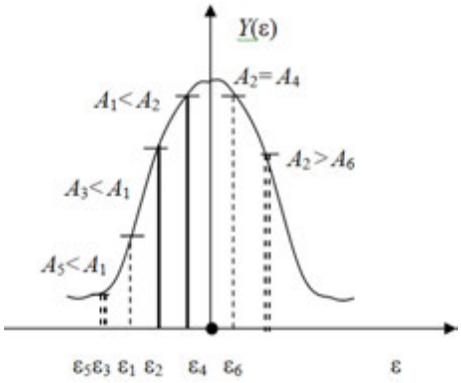

Figure 15. Multiple frequencies probing

At that components A_1, A_2, A_5 lie on the left slope and component A_6 lies on the right. It could be defined from phase characteristics. As far as $A_2>A_6$ what is evident from envelope analysis of that pair cutout by band pass filter we should change the parameters of amplitude phase conversion of probe signal one more time. From equation (25) with E_5=0 and limiting to four components will get multi frequency signal with A_1, A_2, A_3 and A_4, and with A_2=A_4, for example, what corresponds the tuning of that pair to the SMBS gain spectra central wavelength [10].

There are possible three types of analysis: analysis of each component alone (differential analysis), analysis of the envelope of each double frequency pair (integral-differential analysis), and the analysis of energy correlation of all components (integral analysis). All of these methods are possible and correspond to single, two-, and multiple frequencies probing of SMBS gain spectra with limited number of optical band pass filters which are conjugated with detuning frequency between spectral components [8].

In more complex way of searching the spectral center and half width we should solve an equation set with amplitude and phase coefficients. Process of multiple frequencies analysis of SMBS gain spectra consists on solving the following equations set [10]

$$\left[\mathbf{D}\right]=\left[\mathbf{A}\right]\times\left[\mathbf{E}\right]\times\left[\mathbf{E}\right]^{*}, \tag{30}$$

where **[D]** is matrix of output photo detector currents value with frequencies $k\Omega$; **[A]** is matrix describing required SMBS gain spectra components in band $\Delta\omega$; **[E]** is matrix describing

http://dx.doi.org/10.5772/59144

spectrum of probe multiple frequencies oscillation with frequencies $\{\omega_0 \pm k\Omega\}\{\Delta\omega\}$, **[E]** is complex conjugate matrix with [E].

On the first step SMBS gain spectra is probing by two-frequency oscillation, amplitude of the components with $n \geq 3$ equals zero. At the same time hitting the SMBS gain spectra central peak is not required. From the analysis of photo detector components on frequency Ω we can define SMBS gain spectra slope, its steepness, frequency shift from central peak of reflection[8]. During the second step we use multi frequency oscillation, which component with $n=3$ does not equal zero. During the third step we use multi frequency oscillation, which component with $n=3$ equals zero, and component with $n=5$ does not equal zero. At the same time we analyze amplitudes of photo detector components with frequenciesΩ, 2Ω, 3Ω. As far as the amplitude of probe signal components is known and stable, as it has been shown before, we could with given precision define SMBS gain spectra, such as central wavelength, steepness, symmetry of the spectrum curve, and etc. At the third step varying the frequency Ω, number of components n and working filters with frequencies $k\Omega$, we could optimize SMBS gain spectra analysis and tune the central frequency of probe laser to the reflection peak to take a tracking signal [8].

5.4. Some remarks for SNR of spectra characterization

Let's consider some different situations with single, two-, and multiple frequencies probing of real selective structures with limited number of optical band pass filters which are conjugated with detuning frequency between spectral components [8]. SMBS gain spectra characterization from optical to the electrical field by single-sideband amplitude modulated radiation, in which the upper sideband is suppressed and single frequency probing is used in [6]. SMBS gain spectra characterization in single-mode optical fiber was presented in [7]. It is based on the use of advantages of single-sideband modulation and two-frequency probing radiation, which gives possibility of transfer the data signal's spectrum in the low noise region of a photo detector. Two-frequency scanning and multiple frequencies probing of SMBS gain spectra are discussed in sections 4.2-4.3 and were partly considered in [8]. SMBS gain spectra characterization with two-frequency heterodyne and single frequency scanning was discussed in [4].

As we can see from [6,7] the needed bandwidth of photo detector is determined by Mandelstam-Brillouin frequency shift and equal to 10-20 GHz. One version of signal processing may be realized on the envelope of differential frequency $2\Delta f$ [7]. So the needed bandwidth of photo detector is determined by Mandelstam-Brillouin gain and equal to 20-100 MHz. The same value of bandwidth is a feature of methods which are presented now and discussed in [8]. Additional advantage of method [4] is heterodyning. Applying of photo heterodyning allows significantly increase the system sensitivity under the condition of weak signals and receives information from frequency pushing of counter propagated signal spectrum [8].

If we don't go into details of the physical nature phenomena, the basic noises level of the radiance receivers is more than background noises level and determine the detect ability of receiving signal. The gain in SNR relative to single frequency measurements can be calculated as [63]

$$G = \int_0^{\Delta f} S(f)\,df \Big/ \int_{f_0+\Delta f}^{f_0-\Delta f} S(f)\,df \tag{31}$$

where $S(f)$ – spectral density of radiance receiver noises, Δf – bandwidth of photo receiver.

The gain will be determined by different nature and level of noise in different frequency regions (fig. 16)

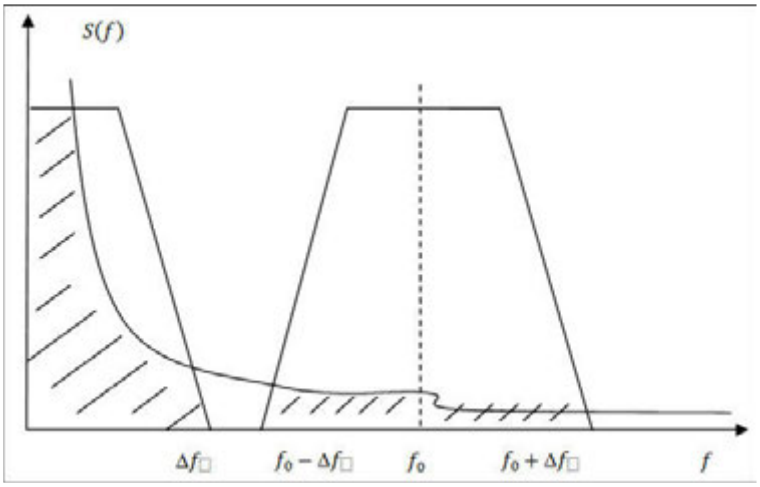

Figure 16. To SNR gain remarks

There are current noises with distribution type 1/*f* and other powerful noises of low frequency nature for region {0...Δ*f*}for variants 2,4. There are thermal agitations and shot noises with low intension for region {f_0 Δ*f*... f_0+Δ*f*} for present methods and heterodyning 9. For little distance routes the gain in SNR can be mount to 1–2 orders. All these summaries are correct and for multiple frequencies probing [8]. The results are much closed to [53].

5.5. Notch filters for suppressing of Rayleigh scattering

The Raman scattering of light is known to be accompanied by the emergence of spectral components shifted in terms of frequency [15]. The number and the spectral positions of these lines depend on the structural characteristics of the scattering medium. It is known that the intensity of the anti-Stokes line is very low (30 dB weaker than the amplitude of elastic Rayleigh scattering); therefore, registration of the ratio of intensities of the Stokes and anti-Stokes components is a difficult task. In addition, the power of the probing radiation should not exceed several watts to avoid such nonlinear effects as the stimulated Raman scattering and the stimulated Mandelstam-Brillouin scattering. The principle of the SMBS distributed temperature sensors is based on the Landau-Placzek ratio where the temperature-insensitive

http://dx.doi.org/10.5772/59144

Rayleigh signal provides a reference measurement of the fiber background losses and the temperature-sensitive Brillouin signal provides a measurement of the temperature [16]. It is estimated that the Rayleigh signal must be suppressed by at least 33 dB to reduce the effects of SRN to an acceptable level. In these circumstances, in order to achieve high accuracy of temperature measurement is required to choose the optimal method of Rayleigh scattering filtration and separation of the desired signal with minimal loss of information.

The separation of the relatively weak Brillouin signal from the Rayleigh has been reported using a bulk Fabry-Pérot interferometer (FPI) [54], which is lossy and expensive. A fiber Mach–Zehnder interferometer (MZI) has been demonstrated to achieve 27-dB Rayleigh rejection using a-switched fiber laser probe of 1.5-GHz bandwidth [55]. However, with a narrow-band source (20 MHz) and the resultant increased coherent Rayleigh noise, this is insufficient to achieve a temperature resolution of 1 °C. In [16] reports on the use of a narrow-band fiber Bragg grating filter (FBGF), which achieves recovery of the Brillouin signal by suppressing the Rayleigh signal. In this way, the Brillouin light path is subject to minimum attenuation and is frequency independent. Typically, the filter uses fiber Bragg gratings that produce narrow-band signals of the Stokes and anti-Stokes components [14], which are then sent on different channels registration. However, this method makes great demands on the quality of lattices: a spectral width (which should be as much as possible), the reflection coefficient, losses, and so on. Unfortunately, even under optimal conditions, a significant portion of the desired signal is lost during filtration. So, FBG is more effective to suppress Rayleigh scattering, then to detail Stokes and anti-Stokes components.

In [14,15] FBG with a spectral width of 0.5 nm reflection used to suppress the central Rayleigh line, which allowed to minimize the noise introduced by Rayleigh scattering without a substantial reduction in the integrated intensity of Raman shift lines. After filtering, the signal components of the SRS were separated by directional couplers with the appropriate wavelengths and sent to pin-photodiodes. It was not possible in [16] to obtain a single grating that would provide rejection of Rayleigh line. Hence, the filter comprises two cascaded gratings separated with an isolator to prevent the formation of an étalon. The rating characteristics were all supplied to the following specifications: bandwidth 0.13 nm, reflectivity 0.98%. In this way the FBG offers minimum attenuation to the two Brillouin sidebands, which, therefore, pass relatively unaffected through the filter.

We developed a new method of FBG writing on the basis of phase mask and restrictive object positioned between mask and fiber. Such optical scheme was realized and we got FBG, which allowed measurements of intensity of the Raman or Mandelstam-Brillouin scattering components in a wide spectral range with the minimum losses; the sensitivity of a conventional InGaAs photo-detector turned out to be sufficient for these measurements. This filter suppressed the central area of the spectrum at the wavelength of 1552,6 nm and transmitted the anti-Stokes and Stokes lines of the Raman or Brillouin scattering. The spectra of FBG for Rayleigh line filtration in SMBS gain spectra characterization, obtained by the spectrum analyzer 5240 FTB-S with a resolution of 2 pm, is shown on fig. 17.

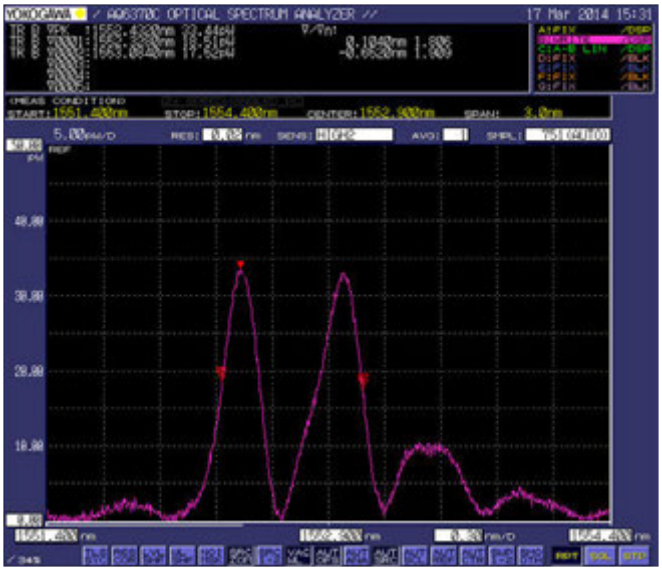

Figure 17. Spectra of FBG filter

Figure 18. Setup for FBG recording

FBG for the experiments was manufactured by a given method of continuous recording with restrictive object in the setup, shown in Fig. 18, at the R&D Institute of Applied Electrodynamics, Photonics and Living Systems. The setup for FBG recording was made in Novosibrsk State University on the base of amplitude-modulated ultraviolet laser with the conversion of the second harmonic on the Ar+. Laser was focused on the core of the aged in hydrogen-doped germanium-silicon fiber (SMF-28).

http://dx.doi.org/10.5772/59144

5.6. Discussion of results

On the basis of two-frequency signal information structure investigation main principles of combined interaction of its instantaneous values of amplitude, phase and frequency with arbitrary contour has been defined. The numerical simulation in dual-drive MZM was carried out and different poly-harmonic spectrums were realized. Novel methods for multiple frequency characterization of stimulated SMBS gain spectrum in single-mode optical fiber are presented. This method is based on the usage of multiple frequencies probing radiation [8]. For conversion of the complex SMBS gain spectra from optical to the electrical field single-sideband modulation, direct or heterodyne detection are used. Determining of a multiple frequencies positions over the gain spectrum occurs through the amplitude modulation index of the envelope or the phase difference between envelopes of probing and passing components. The methods are characterized by high resolution, SNR of the measurements increased of a two order, simplicity of the offered algorithms for finding the central frequency, *Q*-factor and SMBS maximum gain coefficient. Measurement algorithm is realized on simple and stable experimental setup. Applying of photo heterodyning allows significantly increase the system sensitivity under the condition of weak signals and receives information from frequency pushing of counter propagated signal spectrum. We developed a new method of FBG writing on the basis of phase mask and restrictive object positioned between mask and fiber. Such optical scheme was realized and we got FBG, which allowed measurements of intensity of the Raman or Mandelstam-Brillouin scattering components in a wide spectral range with the minimum losses and deep suppression of Rayleigh scattering line.

6. Conclusion

We reviewed the principle and the applications of the poly-harmonic (two-frequency or four-frequency) cw laser systems for characterization of Mandelstam-Brillouin gain contour, Raman scattering contours and FBG reflection spectra. Investigation methods and approaches are based on the unity of resonant structures of generated fiber responses on exciting and probing radiation or external physical fields for all given effects. The main decision is based on poly-harmonic probing of formed resonance responses. A variety of multiplexed measuring functions can be provided by the technique for telecom and sensing applications. As the examples, we introduced new four-frequency methods for Mandelstam-Brillouin gain contour and FBG spectra characterization classified by average and difference frequencies of probing radiation. These systems possess the advantages of the continuous-wave operation, high resolution, high accuracy, and absence of the need to measure the phase characteristics of the tested contours. We proposed for the first time the concept, approaches and methods for its implementation, which allowed reasonably formulate and solve the problem of creation of scientific and technical basis for designing software-defined down-hole fiber optic telemetry systems based on the combination of nonlinear reflectometry (inelastic Raman and Mandelstam-Brillouin, elastic Rayleigh and FBG) with improved metrological characteristics of poly-harmonic probing of sensing structures, including the removal of multiplicative and measurement errors caused by instability of the common source of forming radiations in wide

frequency range. Universal poly-harmonic source of probing radiation, variants of scanning and multiple methods of probing, notch filters for Rayleigh scattering line suppression were demonstrated as elements of perspective systems of given class. Applications of designed methods and means in microwave range were also discussed.

Acknowledgements

This work was financially supported by the Ministry of Education and Science of the Russian Federation in the framework of the basic parts of the state and project assignments for works on the organization of scientific research conducted by Tupolev Kazan National Research Technical University (Kazan Aircraft Institute) at R&D Institute of Applied Electrodynamics, Photonics and Living Systems, and Department of Radiophotonics and Microwave Technologies (program "Photonics", 3.1962.2014K).

Author details

Oleg G. Morozov, Gennady A. Morozov*, Ilnur I. Nureev and Anvar A. Talipov

*Address all correspondence to: gmorozov-2010@mail.ru

Tupolev Kazan National Research Technical University (Kazan Aircraft Institute), R&D Institute of Applied Electrodynamics, Photonics and Living Systems, Department of Radiophotonics and Microwave Technologies, Kazan, Tatarstan, Russia

References

[1] Agrawal GP. Nonlinear Fiber Optics. Fifth Edition. Oxford: Academic Press; 2013.

[2] Vasil'ev SA et al. Fibre gratings and their applications. Quantum Electronics 2005; 35(12) 1085-1103.

[3] Udd E., Spillman WB, Jr. Fiber Optic Sensors: An Introduction for Engineers and Scientists. Hoboken, New Jersy: John Wiley & Sons, Inc.; 2011.

[4] Morozov O. et al. Synthesis of Two-Frequency Symmetrical Radiation and Its Application in Fiber Optical Structures Monitoring. In: Yasin M. (ed.) Fiber Optic Sensors. Rijeka: InTech; 2012. P137-164. DOI: 10.5772/27304. Available from: http://www.intechopen.com/books/fiber-optic-sensors/synthesis-of-two-frequency-symmetrical-radiation-and-its-application-in-fiber-optical-structures-mon (accessed 24 August 2014).

http://dx.doi.org/10.5772/59144

[5] Shibata N. et al. Identification of longitudinal acoustic modes guided in the core region of a single-mode optical fiber by Brillouin gain spectra measurements. Optics Letters 1988; 13(7) 595–597.

[6] Loayssa A. et al. Characterization of stimulated Brillouin scattering spectra by use of optical single-sideband modulation. Optics Letters 2004; 29(6) 638-640.

[7] Morozov O. et al. Characterization of stimulated Mandelstam-Brillouin scattering spectrum using a double-frequency probing radiation. Proceedings of SPIE – The International Society for Optical Engineering 2012; 8787 878709-6.

[8] Morozov O. et al. Principles of multiple frequencies characterization of stimulated Mandelstam-Brillouin gain spectrum. Proceedings of SPIE – The International Society for Optical Engineering 2014; 9156 91560K-7.

[9] Morozov O. et al. Methodology of symmetric double frequency reflectometry for selective fiber optic structures. Proceedings of SPIE – The International Society for Optical Engineering 2008; 7026 70260I-8.

[10] Morozov O. et al. Metrological aspects of symmetric double frequency and multi frequency reflectometry for fiber Bragg structures. Proceedings of SPIE – The International Society for Optical Engineering 2008; 7026 70260J-6.

[11] Morozov O. et al. Instantaneous frequency measurement of microwave signals in optical range using "frequency-amplitude" conversion in the π-phase-shifted fiber Bragg grating. Proceedings of SPIE – The International Society for Optical Engineering 2014; 9136 91361B-8.

[12] Long DA. Raman Spectroscopy. New York: McGraw-Hill; 1977.

[13] Grattan KTV and Sun T. Fiber Optic Sensor Technology: An Overview. Sensors Actuators 2000; A82(1–3) 40–61.

[14] Kuznetsov AG, Babin SA, and Shelemba IS. Distributed Fiber Sensor of Temperature with Spectral Filtration by Distributed Fiber Couplers. Kvant. Elektron. 2009; 39 (11) 1078–1081.

[15] Babin SA, Kuznetsov AG, and Shelemba IS. Comparison of Temperature Distribution Measurement Methods with the Use of the Bragg Gratings and Raman Scattering of Light in Optical Fibers. Optoelectronics, Instrumentation and Data Processing 2010; 46(4) 353–359.

[16] Wait PC and Hartog AH. Spontaneous Brillouin-Based Distributed Temperature Sensor Utilizing a Fiber Bragg Grating Notch Filter for the Separation of the Brillouin Signal. IEEE photonics technology letters 2001; 13(5) 508-510.

[17] Stolen RH, Ippen EP, and Tynes AR. Raman oscillaton in glass optical waveguide. Appl. Phys. Lett. 1972; 20 62-64.

[18] Ippen EP and Stolen RH. Stimulated Brillouin scattering in optical fibers. Appl. Phys. Lett. 1972; 21 539-540.

[19] Walrafen GE and Krishnan PN. Model analysis of the Raman spectrum from fused silica optical fibers. Appl. Opt. 1982; 21(3) 359-360.

[20] Rottwitt K. et al. Scaling of the Raman Gain Coefficient: Applications to Germanosilicate Fibers. J. Lightwave Techn. 2003; 21(7) 1652-1662.

[21] Felinskyi G. Nonlinear fitting of the complex Raman gain profile in singlemode optical fibers. In: 11 Int. Conf. on Mathematical Methods in Electromagnetic Theory, MMKT-06, June 26-29, 2006, Kharkiv, Ukraine. 378-380.

[22] Haijuan J. et al. Stability-improved slow light in polarization-maintaining fiber based on polarization-managed stimulated Brillouin scattering. J. Opt. 2013; 15 035404-5. DOI:10.1088/2040-8978/15/3/035404

[23] Al-Qazwini ZAT, Abdullah MK, Mokhtar MB. Measurements of stimulated-Raman-scattering induced tilt in spectral-amplitude-coding optical code-division multiple-access systems. Optical Engineering 2009; 48(1) 015001-6.

[24] André PS et al. Raman Gain characterization in Standard Single Mode Optical Fibres for Optical Simulation Purposes. http://www.researchgate.net/publication/228357255_Raman_gain_characterization_in_standard_single_mode_optical_fibres_for_optical_simulation_purposes (accessed 24 August 2014).

[25] Ming L. et al. Multichannel notch filter based on phase-shifted phase-only-sampled fiber Bragg grating. Optics Express 2008; 16(23) 19388-19394.

[26] Oliveira Silva SF. Fiber Bragg grating based structures for sensing and filtering. Porto: Porto University; 2007.

[27] Chehura E., James SW, and Tatam RP. A simple method for fabricating phase-shifted fibre Bragg gratings with flexible choice of centre wavelength. Proceedings of SPIE – The International Society for Optical Engineering 2009; 7503 750379-7.

[28] Junfeng J. et al. Investigation of peak wavelength detection of fiber Bragg grating with sparse spectral data. Optical Engineering 2012; 51(3) 034403-5.

[29] Bodendorfer T. et al. Comparison of different peak detection algorithms with regards to spectrometric fiber Bragg grating interrogation systems. In: International Symposium on Optomechatronic Technologies, ISOT-2009, 2009, Istanbul, Turkey. 122-126.

[30] Morozov OG, Aybatov DL. Spectrum conversion investigation in lithium niobate Mach-Zehnder modulator. Proceedings of SPIE – The International Society for Optical Engineering 2010; 7523 75230D-8.

[31] Aybatov DL, Morozov OG, and Sadeev TS. Dual port MZM based optical comb generator for all-optical microwave photonic devices. Proceedings of SPIE – The International Society for Optical Engineering 2011; 7992 799202-7.

[32] Sadeev TS, Morozov OG. Investigation and analysis of electro-optical devices in implementation of microwave photonic filters. Proceedings of SPIE – The International Society for Optical Engineering 2012; 8410 841007-6.

[33] Morozov OG. RZ, CS-RZ and soliton generation for access networks applications: problems and variants of decisions. Proceedings of SPIE – The International Society for Optical Engineering 2012; 8410 84100P-8.

[34] Mao XP, Tkach RW, Chraplyvy AR. Stimulated Brillouin threshold dependence on fiber type and uniformity. IEEE Photon. Technol. Lett. 1992; 4(1) 66–69.

[35] Loayssa A., Benito D., Garde MJ. Optical carrier Brillouin processing of microwave photonic signals. Opt. Lett. 2000; 25(17) 1234-1236.

[36] Honda N. In-Service Line Monitoring for Passive Optical Networks. In: Yasin M. et al. (ed.) Optical Fiber Communications and Devices. Rijeka: InTech; 2012. p203-218.

[37] Oh I., Yegnanarayanan S., Jalali B. High-resolution microwave phonon spectroscopy of dispersion shifted fiber. IEEE Photon. Technol. Lett. 2002; 14(3) 358–360.

[38] Nikles M., Thevenaz L., Robert PA. Brillouin gain spectrum characterization in single-mode optical fibers. J. Lightwave Technol. 1997; 15(10) 1842–1851.

[39] Loayssa A., Benito D., Garde MJ. Narrow-bandwidth technique for stimulated Brillouin scattering spectral characterization. Electron. Lett. 2001; 37(6) 367–368.

[40] Sagues M., Loayssa A. Swept optical single sideband modulation for spectral measurement applications using stimulated Brillouin scattering. Optics Express 2010; 18(16) 17555-17568.

[41] Morozov OG et al. Structural minimization of fiber optic sensor nets for monitoring of dangerous materials storage. Proceedings of SPIE – The International Society for Optical Engineering 2011; 7992 79920E-9.

[42] Petoukhov VM. Two-frequency IR CW LFM LIDAR for remote sensing of hydrocarbons and gas vapor. Proceedings of SPIE – The International Society for Optical Engineering 1997; 3122 339-346.

[43] Morozov OG. Two-frequency scanning LFM LIDARS: theory and applications. Proceedings of SPIE – The International Society for Optical Engineering 2002; 4539 158-168.

[44] Bogdanov NG, Plotnikov SN, Stchekotchihin SN. Monitoring of thickness of not magnetic coverings on a ferromagnetic basis. Factory laboratory. Materials Diagnostic 2007; 12 30-33.

[45] Aybatov DL. Distributed temperature fiber Bragg grating sensor. Proceedings of SPIE – The International Society for Optical Engineering 2009; 7374 73740B-6. DOI: 10.1117/12.829002.

[46] Weaver T. Thermal drift compensation system and method for optical network. Patent WO 020838, 2008.

[47] Jackson RG. Advanced sensors. Moscow: Technosphere; 2007.

[48] Sadykov IR, Morozov OG, Sadeev TS. The biosensor based on fiber Bragg grating to determine the composition of the fuel and biofuel. Proceedings of SPIE – The International Society for Optical Engineering 2012; 8410 84100F-8.

[49] Morozov GA. Application of microwave technologies for increase of efficiency of polymeric materials recycling. In:8th International Conference on Antenna Theory and Techniques, ICATT'11, 2011, Kiev, Ukraine. 321-323.

[50] Dong X. Bend measurement with chirp of fiber Bragg grating. Smart materials and structures 2001; 10 1111-1113.

[51] Denisenko PE, Sadeev TS, Morozov OG. Fiber optic monitoring system based on fiber Bragg gratings. Proceedings of SPIE – The International Society for Optical Engineering 2012; 8410 84100K-6.

[52] Morant M. et al. Dual-drive LiNbO3 interferometric Mach-Zehnder architecture with extended linear regime for high peak-to-average OFDM-based communication systems. Optics express 2011; 19(26) B450-B456.

[53] Xiao Y. et al. Multiple microwave frequencies measurement based on stimulated Brillouin scattering with improved measurement range. Opt. Express 2013; 21(26) 31740-31750.

[54] Wait PC and Newson TP. Landau–Placzek ratio applied to distributed fiber sensing. Opt. Commun. 1996; 122 141–146.

[55] Lees GP et al. Recent advances in distributed optical fiber temperature sensing using the Landau–Placzek ratio. Proceedings of SPIE – The International Society for Optical Engineering 1998; 3541 1–5. doi:10.1117/12.339104.

[56] Morozov O. et al. Two-frequency analysis of fiber-optic structures. Proceedings of SPIE – The International Society for Optical Engineering 2006; 6277 62770E-11.

[57] Morozov OG, Nurgazizov MR, Talipov AA. Double-frequency method for the instantaneous frequency and amplitude measurement. In: 9th International Conference on Antenna Theory and Techniques, ICATT-2013, Odessa, Ukraine, 2013. 381-383.

[58] Morozov OG. et al. Intellectual parachute and balloon systems based on fiber optic technologies. Proceedings of SPIE – The International Society for Optical Engineering 2014; 9156 91560B-8.

[59] Morozov O. et al. Instantaneous microwave frequency measurement with monitoring of system temperature. Proceedings of SPIE – The International Society for Optical Engineering 2014; 9156 91560N-7.

http://dx.doi.org/10.5772/59144

[60] Morozov O. et al. Instantaneous frequency measurement of microwave signals in optical range using "frequency-amplitude" conversion in the π-phase-shifted fiber-Bragg grating. Proceedings of SPIE – The International Society for Optical Engineering 2014; 9136 91361B-8.

[61] Morozov O. et al. Theory of symmetrical two-frequency signals and key aspects of its application. Proceedings of SPIE – The International Society for Optical Engineering 2014; 9156 91560M-11.

[62] Morozov O. et al. Training course and tutorial on optical two-frequency domain reflectometry. Proceedings of SPIE – The International Society for Optical Engineering 2012; 8410 84100Q-9.

[63] Natanson O. et al. Reflectometry in open and fiber mediums: technology transfer. Proceedings of SPIE – The International Society for Optical Engineering 2005; 5854 205-214.